Eindhoven University of Technology

MASTER

The influence of advection and diffusion on the time dependent response of tether particle based biosensors simulated with COMSOL Multiphysics

van Houts, Rens

Award date:
2021

[Link to publication](#)

TU/e EINDHOVEN UNIVERSITY OF TECHNOLOGY

Eindhoven University of Technology
Department of Applied Physics
Molecular Biosensors for medical diagnostics

The influence of advection and diffusion on the time dependent response of tether particle based biosensors simulated with COMSOL Multiphysics

Master Thesis

Author:
Rens van Houts

MBx 2021-3

22-04-2021

Supervised by:

Dr. L.J. van IJzendoorn

ABSTRACT

Biosensors are applied in a wide variety of fields, such as the medical field and the food industry. The presence of specific biomarkers (analyte) can be detected or the concentration of the analyte can be continuously monitored. This thesis focuses on biosensing based on particle mobility (BPM). Visser et al. (2018) experimentally measured that the timescale to reach a stable activity for concentrations in the nM and pM regime is in the order of hours for the BPM sensor. This timescale limits the ability to measure time dependent biomarker concentrations. The aim of the thesis is to investigate the influence of flow, diffusion and reactions on the time dependent analyte concentration between the particles and the surface of the flow cell and the time dependent activity of the BPM sensor.

By carrying out COMSOL simulations with flow and diffusion for a flow cell used in experiments, it was found that the distribution of analyte between the particles and the surface is diffusion dominated. Furthermore it was found that the time required to reach a stable analyte concentration between particles and the surface is in the order of minutes.

By adding reactions between the analyte and binders to the COMSOL simulations, it was found that the timescale required to reach equilibrium can drastically increase to hours for both the local analyte concentration and the activity. For BPM competition assays and sandwich assays it was found that the activity of the BPM sensor in equilibrium is only dependent on the value of K_d. Furthermore, the time required to reach a stable activity increases for a decrease in the value of K_d.

For a BPM competition assay and an increasing analyte concentration it was found that the time required to reach a stable activity for a specific value of K_d decreases for increasing k_{on} values. However, for a typical experimental condition of a flowrate of 30 μL/min and a binding site areal density of 10^{16} /m^2 , the time required to reach a stable activity does not decrease any further for $k_{on} > 10^6$ M^{-1}s^{-1}. For a decreasing analyte concentration it was found that the time required to reach the maximum activity increases for decreasing k_{off} value.

For BPM sandwich assays it was found that the time required to reach equilibrium can drastically increase for concentration in pM an nM regime. The minimum required time to reach equilibrium is the time for the sample to be distributed over the flow cell.

TABLE OF CONTENTS

1 INTRODUCTION

1.1 BIOSENSOR APPLICATION AND MEASUREMENT ASSAYS

Biosensors are devices which can provide quantitative or semi-quantitave analytical information, e.g. the concentration of biomarkers, or analyte, such as proteins, DNA/RNA, antibodies and viruses. [1] Analyte chemically reacts with surface receptors, such as enzymes, aptamers and antibodies. The surface receptors, or binders, are chosen such that a specific analyte can be measured with the biosensor. The chemical reactions are transduced to a measurable physical quantity (e.g. fluorescence or light scattering). The physical quantity, which are dependent on the analyte concentration, can be translated to a numerical output, a signal. Varying concentration will result in varying signal. By interpreting the signal qualitative and sometimes quantitative statements can be made. [2] [3]

Biosensors are applied in a wide variety of fields, like the medical field and the food industry. [4] In the medical field biosensors are used for diagnosing patients, for example. Glucose biosensor are widely used for the diagnosis of diabetes mellitus. [5] In the food industry biosensors are used for monitoring food quality and safety. Pesticides, for example, are toxic for the environment and humans. [6] Countries have made legislations on the maximum residue level of pesticides in food. [7] By measuring the pesticide level in food, the food safety can be regulated. [8]

The diagnosis of patient by measuring a decease specific biomarker is an example of a one-time measurement. For a one-time measurement the concentration or presence of a biomarker is determined for a specific moment. However, biosensor can be used for continuous measurements. An example is the continuous measurement of glucose. A continuous glucose measurement device can alarm the patient for hypoglycemia, low glucose levels in blood, and hyperglycemia, high glucose levels in blood. Continuous glucose measurement devices are especially important for patient who have hypoglycemia unawareness. [9]

1.2 MEASUREMENT OF ANALYTE

1.2.1 Competition assay

In this section analyte measurement with a competition assay will be introduced. In figure 1.1A a schematic overview of a competition assay is given. In a competition assay capture molecules, binders, are immobilized to the surface of the sensor. A sample containing analyte molecules is flown into the sensor. The analyte molecules will react with the binders. An analog is added to the sample, which will compete with the analyte to react with the binders. Analog and analyte molecules will react with the binders, such that a binder can only be reacted with either an analyte molecule or analog. The analog concentration is known and the measured signal is dependent on the amount of analog that has reacted with the binders. The amount of analog that has reacted with the binders depends on the analyte concentration, since analog and analyte are in competition to react with binders.

The competition assay that will be discussed in this paper is based on tether micro-particles. Micro-particles are attached to the surface of the sensor by a DNA tether. The analog molecules are immobilized on the surface of the particle. Extra bonds can be formed between the particle and the surface of the sensor. The particle can bind and unbind from the surface, by use of reversible, affinity based reaction. In figure 1.1B the bound and unbound state of the particle is illustrated. The output of this sensor is the activity. Activity is defined as the number of observed switches per particles per unit of

4

time. Analyte molecules will block off binders, such that the activity of the sensor decreases for increasing analyte concentration.
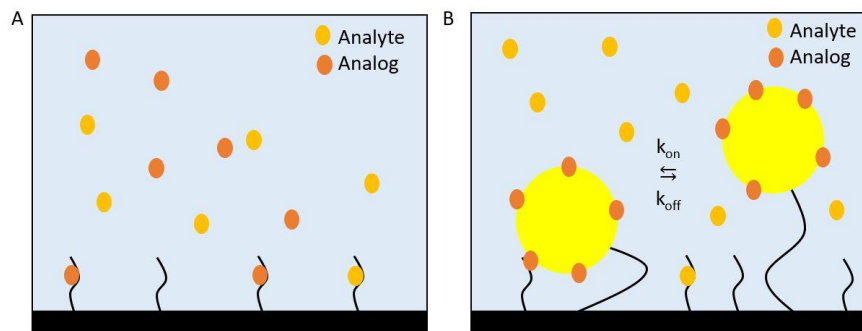

Figure 1.1: (A) Schematic sketch of a competition assay. Binders (black) are immobilized on the surface. Analyte (yellow) and analog molecules (orange) are competing to react with the binders. (B) Schematic sketch of a competition assay with tether particles (bright yellow). Analog (orange) is immobilized on the surface of the particles. The particle switches between the bound state (left) and unbound state (right).

1.2.2   Sandwich assay

In this section the sandwich immunoassays will be introduced. In figure 1.2A a schematic overview of a sandwich immunoassay is illustrated. In a sandwich assay binders are immobilized at the surface of the sensor. A sample containing analyte molecules as well a second type of binders is flown into the sensor. The binders on the surface react to a different part of the analyte than the binders in the sample. A signal is produced when a sandwich is formed. A sandwich is formed when an analyte molecule has reacted with a binder on the surface and a binder on the sample.

The sandwich assay that will be discussed in this paper is based on tether micro-particles. Particles are attached to the surface of the sensor by a DNA tether. Binders are immobilized on the surface of the sensor, but also on the surface of the particle. No binders are present in the sample. A particle can form a bond with the surface when an analyte molecule has reacted with a binder on the surface and a binder on the surface of the particle. The reaction of analyte with the binders on the surface and the reaction of analyte with binders on the particle are both reversible, affinity based reaction. This allows particles to bind and unbind from the surface as illustrated in figure 1.2B. As for the competition assay, an activity can be measured, which is defined as the number of observed switches between motion patterns per number of observed particles per unit of time.

A high affinity based reaction is chosen for the binders on the particle and a low affinity based reaction is chosen for the binders on the surface. [10] For increasing analyte concentration the more binders on the surface will react with analyte, which increases the activity. When the analyte concentration is increased further, more binders on the surface will react with analyte as well which will result in a drop of activity.
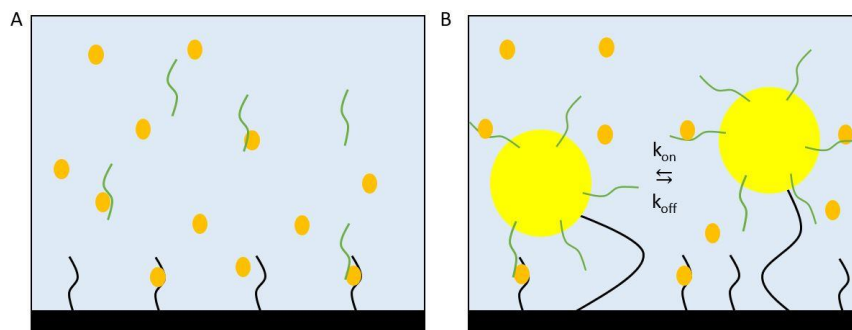
Figure 1.2: (A) Schematic sketch of a sandwich assay. Binders (black) are immobilized on the surface. Analyte (yellow) can react with binders on the surface and a second binder (green). A sandwich is formed when an analyte molecule reacts with both binders at once. (B) Schematic sketch of a sandwich assay with tether particles (bright yellow). Binders are immobilized on the surface (black) and a second binder is immobilized on the particle (green). The particle switches between the bound state (left) and unbound state (right).

1.3 BPM SENSOR

The principle of biomarker monitoring based on the sensing of particle mobility (BPM) is integrated in a micro fluidic flow cell. [10] The BPM sensor can be used for continuously monitoring of a time varying analyte concentration with single molecule resolution. The sensor consists of a micro fluidic flow cell and does not consume analyte or binders, since affinity based, reversible reactions are used. Within the sensor micro-particles are attached to the bottom surface of the flow cell by a flexible DNA tether. The switching between bound and unbound state can be detected by tracking the movement of the particle. The motion pattern of unbound particle is pancake shaped, due to the confinement of the tether. [23] A small motion pattern is observed, when a bond has formed between the surface and the particle, since the length of the bond is shorter than the length of the tether. The change between motion patterns can be observed by use of microscope. The movement of the particles is digitally processed to determine whether a particle is in the bound or unbound state. [10] [18] [23]

1.4 PROBLEM STATEMENT AND AIM OF THE PROJECT

Visser et al. (2018) have performed continuous measurements of BPM sandwich assays. Measurements were performed in which the analyte concentration was increased in a stepwise fashion over three orders of magnitude in pM and nM regime. Every 15 min the analyte concentration was increased and the activity was measured for 5 min. The measured activity was compared to a model which uses first order reaction kinetics of the interaction between analyte molecules and binders. When the measured experimental activities were compared to the calculated activities, it was found that the assay was not in a thermodynamic equilibrium, but in a kinetic regime, when the activity of the system was measured. This meant that the timescale on which the assay would reach thermodynamic equilibrium is longer than the time between the increases of the concentration.

After the series of stepwise increase a sample with no analyte molecules was flown into the sensor. The analyte concentration in the flow cell is kept at zero for 150 min. The activity was measured every 30 min, to investigate the decrease of the activity. The activity decreases due to the dissociation of analyte molecules with the binders. Dissociated analyte molecules will diffuse away from the surface. It was found that the activity decreases over a longer time period than the dissociation time of the analyte with the binders found in literature. A possible explanation is that the local analyte concentration

6

between particles and the surface is in the µM, mM regime (for pM and nM measurements). This can cause rebinding of analyte molecules with binders, which slows down the decrease of the activity.

The aim of the thesis is to investigate the influence of flow, diffusion and reactions on the time dependent analyte concentration between tethered particles and the surface, and the time dependent activity of the BPM sensor.

A model will be developed in COMSOL Multiphysics, to investigate the influence of advection and diffusion on the time dependent analyte concentration in the BPM flow cell and between particles and the surface.
Furthermore, the model will be extended with affinity based reactions between analyte and binders. The influence of the reaction parameters k_{on}, k_{off} and K_d on the local analyte concentration, but also the time dependent activity will be studied. Lastly the timescale on which equilibrium for a variety of BPM competition and sandwich assays for increasing analyte concentrations will be determined.

2 THEORY

In this chapter the theoretical background will be discussed of transport of a sample with analyte in the BPM flow cell and the reaction of analyte with binders. The expression given in this chapter will be used to validate the FEM model calculations of the flow cell described in chapter 6. Flow in the micro fluidic system will be discussed in sections 1.1-1.3. Analyte transport by advection and diffusion will be discussed in section 1.4. The reactions of the analyte with binders is discussed in section 1.5. The depletion zone is discussed in section 1.6 and the time scale to reach equilibrium in the BPM system is discussed in section 1.7. Lastly, the activity based on the fraction of free binding sites is disused is section 1.8.

2.1 REYNOLDS NUMBER

The fluid transport in the BPM flow cell can be characterized by use of the Reynolds number. The Reynold's number is a dimensionless number and is given by

$$Re = \frac{\rho \, v \, L_d}{\mu},$$

(1)

where ρ represents the fluid density, v the average flow velocity, L_d a characteristic length, and μ the dynamic viscosity. For a microfluidic channel, the characteristic length is usually described by the hydraulic diameter which is given by

$$L_d = \frac{4A}{P},$$

(2)

with A the cross-section of the channel and P the wetted perimeter. For $Re < 2300$ a laminar flow occurs and for $Re > 2900$ turbulent flow is expected. The BPM flow cell has a square cross-section of 5mm by 250μm, while typical flow rate during continuous monitoring are on the order of 30μL/min. This gives a typical Reynold's number on the order of 1 for the BPM flow cell. The flow in the BPM flow cell can be characterized as a laminar flow. In steady state, laminar flow is described as a Poiseuille flow.

2.2 POISEUILLE FLOW

The BPM flow cell will be simulated by use of FEM modeling. To verify the simulated flow an analytical solution of a Poiseuille flow through a square channel will be given. A Poiseuille flow is a steady-state laminar flow in a long rigid channel, which is driven by a pressure difference over the ends of the channel. For a channel with a constant cross-section it is assumed to be translation invariant. It is an analytical solution of the Navier-Stokes equation. The Navier-Stokes equation for incompressible fluids is given by

$$\rho \frac{\partial \vec{v}}{\partial t} + \rho (\vec{v} \cdot \nabla) \vec{v} = \rho \vec{g} - \nabla p + \mu \nabla^2 \vec{v},$$

(3)

with ρ the density of the fluid, $\vec{v}$ the local velocity, $\vec{g}$ the gravitational constant and p the pressure. For a laminar flow equation 3 simplifies to

$$\mu \nabla^2 \vec{v} = \nabla p.$$

(4)

The gravitational force is balanced out by a hydrostatic force, so these forces are left out. The flow is a steady-state flow, thus the velocity is time independent. When the length of the channel is taken parallel to the x-axis, the Navier-Stokes equation, in Cartesian coordinates, is simplified to

8

$$\mu[\partial_y{}^2 + \partial_z{}^2]v_x(y,z) = \partial_x p(x). \tag{5}$$

The cross-section of the flow cell is rectangular, thus an analytical solution of equation 5 for rectangular cross-section is needed, such that the simulated velocity profile can be verified. The solution for the velocity profile in a channel with a rectangular cross-section

$$v_x(y,z) = \frac{4h^2\Delta p}{\pi^3\mu L} \sum_{n,odd}^{\infty} \frac{1}{n^3}\left[1 - \frac{\cosh\left(n\pi\frac{y}{h}\right)}{\cosh\left(n\pi\frac{w}{2h}\right)}\right]\sin\left(n\pi\frac{z}{h}\right), \tag{6}$$
$$for -\frac{1}{2}w < y < \frac{1}{2}w, 0 < z < h,$$

with w the width and h the height of the flow cell. [11] The flow rate is then given by

$$Q = \int_{-\frac{1}{2}w}^{\frac{1}{2}w} dy \int_0^h dz\ \vec{v}_x(y,z),$$

$$Q = \frac{h^3 w\Delta p}{12\mu L}\left[1 - \sum_{n,odd}^{\infty}\frac{1}{n^5}\frac{192}{\pi^5}\frac{h}{w}\tanh\left(n\pi\frac{w}{2h}\right)\right]. \tag{7}$$

The boundary condition that will be used in the FEM simulations is not a pressure gradient, Δp, but a flow rate. Therefore the flow velocity needs to be expressed in terms of the flow rate. The sum in equation 7 can be eliminated by taking the limit of $h/w \to 0$, of a very wide but flat channel. The formula for the flow rate becomes

$$Q \approx \frac{h^3 w\Delta p}{12\mu L}\left(1 - 0.630\frac{h}{w}\right). \tag{8}$$

The error of this approximation for the BPM flow cell, which has an aspect ratio of $h/w = 0.05$ is in the order of $10^{-27}\%$.
This gives the following expression for the velocity profile

$$v_x(y,z) = \frac{48}{\pi^3}\frac{Q}{hw\left(1 - 0.630\frac{h}{w}\right)}\sum_{n,odd}^{\infty}\frac{1}{n^3}\left[1 - \frac{\cosh\left(n\pi\frac{y}{h}\right)}{\cosh\left(n\pi\frac{w}{2h}\right)}\right]\sin\left(n\pi\frac{z}{h}\right). \tag{9}$$

The velocity profile that is produced in the simulation can be verified with equation 9.

Velocity profile close to the surface
In the center of the flow cell close to the bottom surface the effect of the side walls can be neglected. Therefore the solution for a laminar flow between two plates can be used. The velocity profile is given by

$$v_x(z) = \frac{\Delta p}{2\mu L}(h - z)z, \tag{10}$$

and the flow rate by

9

$$Q = \frac{h^3 w}{12\mu L} \Delta p. \tag{11}$$

Close to the surface wall the velocity profile can be approximated to be linear. By substituting equation 11 into equation 10, the velocity profile close to the surface is given by

$$v_x(z) = 6\frac{Q}{h^2 w} z. \tag{12}$$

The velocity profile from equation 12 will be used later in section 1.6.

2.3 VORTICITY

As described in the introduction, micro particles are present in the BPM flow cell. These particles will disturb the flow locally. To determine the range on which a particle disturbs the flow the vorticity will be used. Vorticity is a measure of the rotation of a fluid element as it moves through the flow. The vorticity, $\vec{\omega}$, is defined as the curl of the velocity field $\vec{v}$:

$$\vec{\omega} \equiv \nabla \times \vec{v}. \tag{13}$$

The vorticity describes the change of the velocity vector perpendicular to the velocity. For a laminar flow in the x-direction $\vec{\omega}_x = 0$ holds. A particle will change the flow direction and also the direction of the flow velocity, then $\vec{\omega}_x \neq 0$. Also the y- and z-component of the vorticity will change due to the influence of the particle on the flow.

10

2.4 TRANSPORT BY ADVECTION AND DIFFUSION

Transport of analyte is influenced by advection and diffusion. The transport of analyte is therefore described by the advection-diffusion equation. For a constant diffusion coefficient the advection-diffusion equation is given by

$$\frac{\partial c}{\partial t} = D\nabla^2 c - \nabla \cdot \vec{v}c + R, \tag{14}$$

with c the analyte concentration and R a source term. In the remainder of this section the source term is taken zero.

In context of the BPM advection is the distribution of analyte molecules by a flow. In order to investigate the relative importance of diffusion and advection either two terms of equation 14 can be neglected. By neglecting diffusion, the description of analyte by advection simplifies to:

$$\frac{\partial c}{\partial t} = -\nabla \cdot \vec{v}c. \tag{15}$$

Analyte will be transported linear in time parallel to the flow direction. When a no-slip boundary condition is applied to the walls of the flow cell, a flow velocity at the walls is zero, no analyte will be transported by advection to the walls. Since advection occurs parallel to the flow direction, the analyte will be transported along the stream lines. Streamlines are tangent to the flow velocity. The streamlines can be derived from the stream function which is defined as

$$\vec{v} = \nabla \times \vec{\psi}, \tag{16}$$

with $\vec{\psi}$ the stream function. The stream function can also be derived from the vorticity with

$$\nabla^2 \vec{\psi} = \vec{\omega}. \tag{17}$$

As mentioned before, micro particles are present in the BPM flow cell. Since a particle will have influence on the flow, and thus also on the velocity profile and the vorticity, equation 17 shows that vorticity can be used to determine the influence of the particle on the stream lines and hence it can be used to determine the distance on which the influence of the particle stretches in the fluid flow.

The relative importance of diffusion can be estimated by setting the flow velocity to zero and equation 14 simplifies to

$$\frac{\partial c}{\partial t} = D\nabla^2 c, \tag{18}$$

which describes freely diffusing particles driven by a concentration gradient. The particles will diffuse from regions of high concentration to regions with low concentration.

Since the transport is driven by advection and diffusion, the Péclet number, a dimensionless number, will be introduced, which characterize whether transport or mixing of analyte is advection driven or diffusion driven.

The Péclet number is defined as the time to diffuse over a characteristic length, L, divided by the time to flow over a characteristic length. For the BPM flow cell characteristic lengths are the height of the flow cell, the length of the flow cell and the particle radius. The Péclet number is given by

$$Pe = \frac{t_{diffusion}}{t_{advection}} = \frac{UL}{D},$$

(19)

with U the average flow velocity and D the diffusion coefficient of the analyte. For $Pe \gg 1$ transport is dominated by advection and for $Pe \ll 1$ transport is dominated by diffusion. The Péclet numbers will be explained in more detail section 1.6.
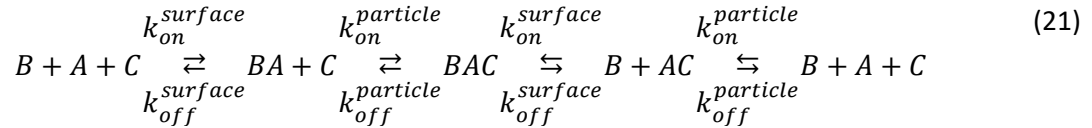
12

2.5 REACTIONS

Since the purpose of this thesis is to investigate the influence of flow and diffusion on a BPM assay the kinetics of reactions between the analyte and binders will be summarized. In the BPM sensor affinity based reversible reaction are used. The reaction between analyte, A, and binders, B, reads

$$A + B \underset{k_{off}}{\overset{k_{on}}{\rightleftarrows}} AB, \tag{20}$$

with AB a binder-analyte complex. The reaction parameters k_{on} and k_{off} are the association rate constant and the dissociation rate constant respectively. In a competition assay analyte will only react with binders present at the surface of the BPM flow cell. Hence equation 20 can be used to described the reaction present in the BPM competition assay, as described in section 1.3.

For sandwich assays, in which both the surface of the BPM flow cell and the particles are covered with binders, an extension of equation 20 must be used. The reaction equations for a sandwich assay is are represented by:

$$B + A + C \underset{k_{off}^{surface}}{\overset{k_{on}^{surface}}{\rightleftarrows}} BA + C \underset{k_{off}^{particle}}{\overset{k_{on}^{particle}}{\rightleftarrows}} BAC \underset{k_{off}^{surface}}{\overset{k_{on}^{surface}}{\leftrightharpoons}} B + AC \underset{k_{off}^{particle}}{\overset{k_{on}^{particle}}{\leftrightharpoons}} B + A + C \tag{21}$$

with, B the binders on the surface of the flow cell and C the binders on the particle and BAC the sandwich where a single analyte molecule is bound with a binder on the surface and a binder on a particle. The sandwich can be formed by either reacting with the surface first and then with the particle or vice versa.

When analyte molecules are reacting with the binders at the surface of the flow cell, the local concentration in the fluid near the surfaces decreases, which is called the depletion zone. The depletion zone is described in more detail in section 3.6. In this section the depletion zone is neglected, the concentration near the surface remains the analyte concentration. With this assumption the reaction can be described by first-order Langmuir kinetics. The number of binding site bound with analyte, $b(t)$, evolves over time as

$$\frac{\partial b}{\partial t} = k_{on} c_s (b_m - b) - k_{off} b, \tag{22}$$

with b_m the binding site areal density, c_s the concentration at the surface. Since the assumption was made that the concentration at the surface remains the analyte concentration c_0, $c_s = c_0$. Equation 22 can be solved to

$$\frac{b(t)}{b_m} = \frac{c_0}{K_d + c_0} \left(1 - e^{-(k_{on} c_0 + k_{off})t} \right), \tag{23}$$

with $K_d = \frac{k_{off}}{k_{on}}$ the dissociation constant. The dissociation constant corresponds to the analyte concentration at which half of the binders reacts in equilibrium. In equation 23 $\frac{b(t)}{b_m}$ represent the fraction of binding sites reacted with analyte. For $t \to \infty$ the fraction of reacted binding sites is constant

and becomes equal to $\frac{c_0}{K_d+c_0}$. When the fraction of reacted binding sites is constant an equilibrium is reached and the measured fraction is related to the analyte concentration in the fluid.

2.6 DEPLETION ZONE

When analyte molecules are reacting with the binders at the surface the local analyte concentration in the fluid decreases. This can induce a temporarily local depletion zone. In this section the size of the depletion zone for the BPM will be discussed. Squires et al. (2008) have done an analysis on depletion zones for surface reactions under flow conditions. [12]

In this section the limiting case, in which analyte immediately reacts with binders upon reaching the surface, will be investigated. Additionally, it is assumed that there is an infinite amount of binding sites at the surface and that analyte remains bound. The depletion zone is then only dependent on the flow rate and the size of the reactive surface.

In the limit of very low flow rates all analyte is able to be transported to the reactive surface. This will create a depletion zone extending over the height of the flow cell and also upstream. The depletion zone will always extend upstream when the time to diffuse from the top of the flow cell to the reactive surface is shorter than the time to flow over the same length. In the limit of very high flow rates the depletion zone will form a layer above the surface, however, it will not extend over the height of the flow cell. To determine in which limit the BPM system operates a Péclet number will be introduced, in which the characteristic length scale is taken to be the height of the flow cell. This Péclet number is given by:

$$Pe_H = \frac{h^2/D}{h^2w/Q} = \frac{Q}{Dw}, \tag{24}$$

with h the height of the flow cell, D the diffusion coefficient of the analyte, w the width of the flow cell and Q the flow rate. For $Pe_H \ll 1$ the depletion zone extends up-stream into the flow cell. All analyte molecules from the sample diffuse to the surface and no analyte molecules are lost. For $Pe_H \gg 1$ the depletion zone is thinner than the height of the flow cell. Only a fraction of the analyte in the sample diffuse to the surface and reacts with the binders.

The width of the BPM flow cell is 5mm. During continuous monitoring a typical flow rate of 30µL/min is used. For a diffusion coefficient of 10^{-10}m²/s, $Pe_H = 1000$ is found to be a typical value for the BPM flow cell. That implies that even in the limit for analyte immediately reacting with binders at the surface, the depletion zone does not extent over the full height of the flow cell. The depletion zone is formed as a layer above the surface. Due to the high flow rate the depletion zone in the BPM flow cell is thinner than the height of the flow cell. This implies that only a fraction of the analyte in the sample reacts with the binders.

In the limiting case for high Pe_H, analyte molecules in the depletion zone experience flow velocities close to the surface. The velocity profile can be approximated and is given by equation 12. A Péclet number can be introduced to relate the depletion zone size with the size of the reactive surface. The second Péclet number is defined as

$$Pe_s = \frac{l^2/D}{h/v_x(h)} = 6\lambda^2 Pe_H, \tag{25}$$

with $v_x(h)$ the flow speed at height h, and $\lambda = \frac{l}{h}$, whit l the length of the reactive surface in the flow direction and h the height of the flow cell. For $Pe_s \gg 1$ the depletion zone is thin compared to the length of the sensing surface, for $Pe_s \ll 1$ the depletion zone is thick compared to the length of the sensing surface. With the Péclet numbers introduced by equation 24 and 25 the size of the depletion zone, δ, can be approximated. [12] The size can be determined as follows

$$\delta \sim \begin{cases} h/Pe_H, for\ Pe_H \leq \lambda \\ l/Pe_s^{1/3}, for\ Pe_H > 1, Pe_H > \lambda\ and\ Pe_s > 1 \\ l/Pe_s^{1/2}, for\ Pe_H > 1\ and\ Pe_s < 1. \end{cases} \qquad (26)$$

Figure 2.1 illustrates different regimes for different Péclet numbers. The subfigures 2.1A and B show the regime in which the flow rate is sufficiently low $Pe_H < 1$ such that all analyte can diffuse to the surface and react. The depletion zone extents upstream and has a size of $\delta \sim h/Pe_H$. Subfigure 2.1D also shows a depletion zone that extents upstream. The flow rate is sufficiently slow and the sensing surface sufficiently large such that all analyte molecules can be collected by the surface. In subfigure C, E and G the depletion zone the flow rate is high, $Pe_H > 1$ which causes a depletion zone thinner than the channel and thin compared to the length of the reactive surface, $Pe_s > 1$. The size of the depletion zone is $\delta \sim l/Pe_s^{1/3}$. For subfigure F the depletion zone is thinner than the channel height, $Pe_H > 1$, but due to the small length of the channel, $Pe_s < 1$ the depletion zone is thick compared to the length of the reactive surface. The size of the depletion zone is $\delta \sim l/Pe_s^{1/2}$.

As stated in the introduction both the surface of the flow cell, with a length of 3cm, and the particles, with a radius of 500nm, can be reactive. For the surface $Pe_s \approx 10^9$ is found and for a particle $Pe_s \approx 10^{-2}$ is found. The depletion zone caused by the surface of the flow cell is thin compared to the height of the flow cell, $Pe_H \gg 1$, and the length of the reactive surface, $Pe_s \gg 1$. It can be compared to the depletion zone shown in figure 2.1E. Only a fraction of the analyte molecules in the fluid are transported to the surface and are able to react with binders. The depletion zone caused by a particle is thin compared to the height of the flow cell, $Pe_H > 1$, but thick compared to the radius of the particle, $Pe < 1$. The depletion zone can be compared to the depletion zone shown in figure 2.1F.

For the reactive surface of the BPM flow cell a size of $\delta \sim 68\mu m$ is found and for a particle a size of $\delta \sim 3.3\mu m$ is found. This implies that for a sandwich assay in a BPM flow cell all particles are present within the depletion zone of the reactive surface of the BPM flow cell, also particles position within a range of $\sim 6.6\mu m$ have overlapping depletion zones. Analyte molecules, within an area where two or multiple depletion zone overlap, are able to be transported to both surfaces.
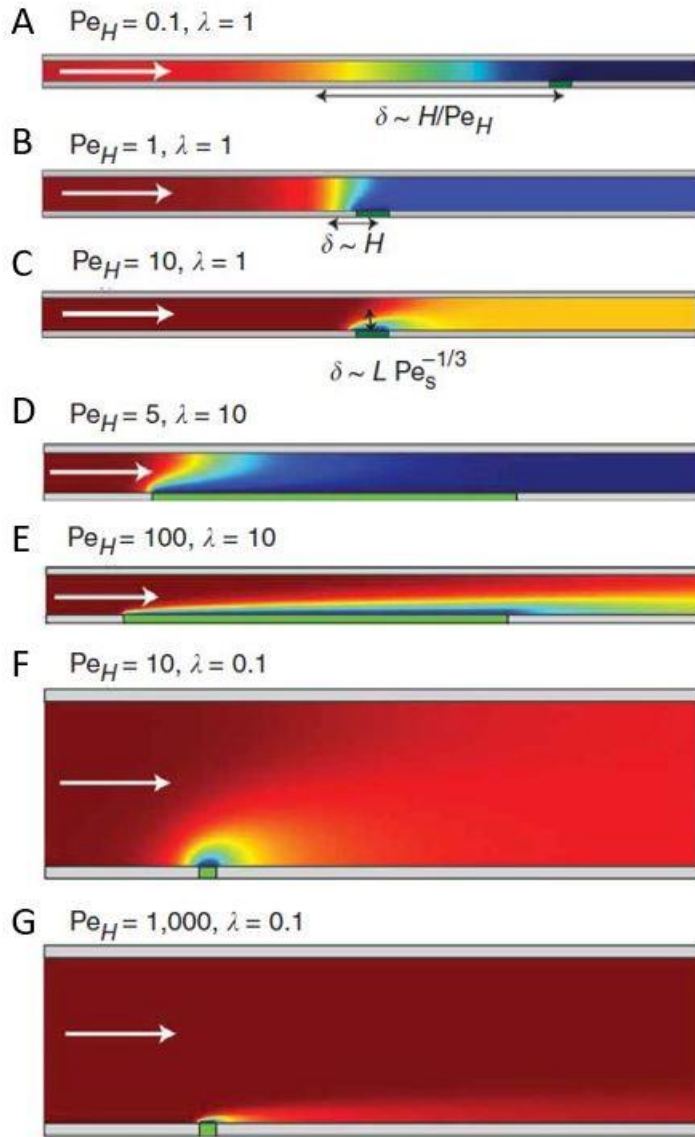
A $Pe_H = 0.1, \lambda = 1$

$\delta \sim H/Pe_H$

B $Pe_H = 1, \lambda = 1$

$\delta \sim H$

C $Pe_H = 10, \lambda = 1$

$\delta \sim L\, Pe_s^{-1/3}$

D $Pe_H = 5, \lambda = 10$

E $Pe_H = 100, \lambda = 10$

F $Pe_H = 10, \lambda = 0.1$

G $Pe_H = 1,000, \lambda = 0.1$

Figure 2.1: Depletion zone for different values of Pe_H and $\lambda = l/h$. In subfigure A, B and D the flow rate is sufficiently low and the reactive surfaces are sufficiently large such that all analyte can diffuse to the surface and react. The depletion zone extents upstream and has a size of $\delta \sim h/Pe_H$. In subfigure C, E and G the depletion zone is thinner than the channel height and thin compared to the reactive surface's length. The size of the depletion zone is $\delta \sim l/Pe_s^{1/3}$. For subfigure F the depletion zone is thinner than the channel height but thick compared to the reactive surface's length. The size of the depletion zone is $\delta \sim l/Pe_s^{1/2}$. The white arrows depict the flow direction. The reactive surface have the same width as the channels. Retrieved from Squires et al. [12].

2.7 TRANSPORT AND REACTION TIMES

In equilibrium the fraction of reacted binding sites relates to the analyte concentration of the sample. In equilibrium the fraction of reacted binding sites is constant. The time to reach equilibrium is dependent on the reaction, but also on the transport of analyte to the reactive surface. In this section the timescale on which equilibrium will be reached under advection (convection), reaction and diffusion, τ_{CRD}, will be discussed.

In the limited of no depletion zone, the time to reach equilibrium is only dependent on the reaction kinetics. The time constant on which the reaction reaches equilibrium, τ_r, follows from equation 23 and is given by:

$$\tau_r = \frac{1}{k_{off} + k_{on}c_0}. \tag{27}$$

However in the BPM system there is a depletion zone, as described in section 2.6. The time constant on which equilibrium is reached depends on the time it takes to transport a sufficient amount of analyte to the surface, such that the reaction reaches equilibrium. This implies that transport will contribute to the time required to reach equilibrium as well. To determine the contribution of transport to the time at which equilibrium is reached a dimensionless number will be introduced, the Damköhler number. The Damköhler number is defined as the reaction rate over the analyte transport rate. The definition used by Squires et al. will be used. [12] This definition is used for affinity based reactions and for reactive surfaces. Since affinity based reaction are also used in the BPM flow cell, the definition introduced by Squires et al. can be used. Squires et al. uses the Damköhler number to determine the time constant on which equilibrium is reached. The Damköhler number is defined as

$$Da = \frac{k_{on}b_m l}{D\mathcal{F}}, \tag{28}$$

with b_m the binding site areal density in mol/m² and $\mathcal{F}$ a dimensionless flux, which is dependent on the Péclet number, Pe_s, from equation 25. The dimensionless flux is the maximum amount of analyte that is transported by the flow to the surface in the limiting case for which all analyte immediately reacts with binders upon arrival at the surface. This dimensionless flux is defined as:

$$\mathcal{F} \approx \begin{cases} 0.81Pe_s^{1/3} + 0.71Pe_s^{-1/6} - 0.2Pe_s^{-1/3} \dots \; for \; Pe_s \gg 1, [13] \\ \pi\left(\ln\left(\frac{4}{Pe_s^{1/2}}\right) + 1.06\right)^{-1} \; for \; Pe_s \ll 1. [14] \end{cases} \tag{29}$$

For $Da \ll 1$ the time dependent response of the BPM is reaction limited, the transport rate of anlyte to the surface is larger than the reaction rate. The timescale to reach equilibrium is limited by only the reaction and will be equal to τ_r. For $Da \gg 1$ the time dependent response of the BPM is transport limited, the transport rate of analyte to the surface is smaller than the reaction rate. The timescale to reach equilibrium is limited by both transport and reaction. In figure 2.2 the relation between the equilibrium time for the BPM system, Damköhler number and the reaction time is plotted. For $Da \gg 1$ the time to reach equilibrium is equal to $\tau_r Da$. The time constant to reach equilibrium in the BPM system is then defined as:

17

$$\tau_{CRD} \sim \begin{cases} \tau_r, for\ Da < 1 \\ \tau_r Da, for\ Da > 1, \end{cases} \qquad (30)$$

with CRD standing for convection (advection), reaction and diffusion. A BPM competition assay, as described in the introduction, has a typical binding site areal density of 10^{16} site/m² and $k_{on} = 10^6$ M⁻¹s⁻¹. The length of the flow cell is 3 cm, with $Pe_s \approx 10^9$. A typical diffusion coefficient for bio molecules is 10^{-10} m²s⁻¹. The Dahmköhler number for a BPM competition assay is $Da \approx 14$. This implies that the BPM flow cell is transport. This implies that the BPM competition assay reaches equilibrium with a time constant of $\tau_{CRD} \sim \tau_r Da$.

The times from equation 30 can be used to estimate the timescale on which the BPM flow cell reaches equilibrium for different assays and concentrations.
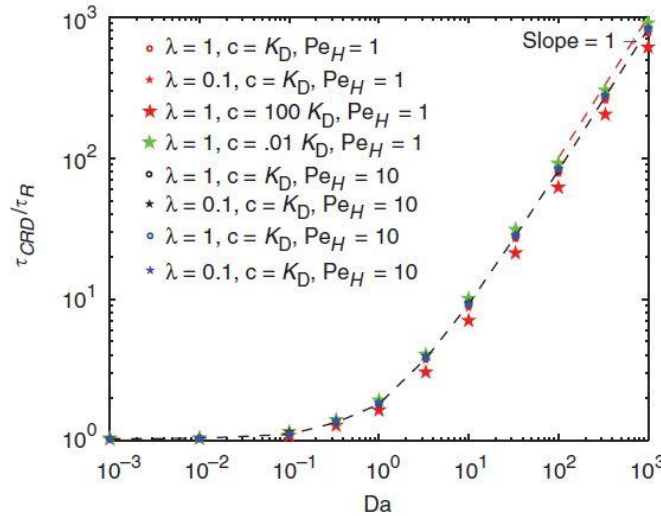

Figure 2.2: Plotted the time scale τ_{CRD} normalized with τ_r for different Damköhler number, Da. For $Da \ll 1$ the system is limited by the reaction. The time to reach equilibrium is only dependent on the time scale of the reaction; $\tau_{CRD} \sim \tau_r$ For $Da \gg 1$ the system is limited by the transport of analyte. The time to reach equilibrium is then $\tau_{CDR} \sim \tau_r Da$. A vast range of different concentration and flow rates collapses on the same curve. Retrieved from Todd M. Squires et al.. [12]

2.8 ACTIVITY

The activity in the BPM flow cell is determined by the binding and unbinding of particles to the surface, as described in the introduction. The measured activity depends on many factor such as particle size, tether length, binding site areal density etc. The activity given in this section is assumed to be proportional to the fraction of free binding sites at the surface. The chance for a reaction between the surface and the particle is proportional to the fraction of free binding sites. The fraction of free binding sites is given by

$$\theta = \frac{b_{free}}{b_{tot}}, \tag{31}$$

with b_{free} the number of free binding sites and b_{tot} the total number of binding sites that are able to react.

First the activity for a competition assay will be discussed. For an analyte concentration of zero the relative activity is 1 and all binding sites are free, $\theta = 1$. For a high analyte concentration the activity is zero and all binding sites react with analyte. No binding site are free, thus $\theta = 0$. This gives the following for the activity:

$$Activity \propto \theta. \tag{32}$$

The activity for a BPM sandwich assay, as described in the introduction, is dependent on the fraction of free binding sites on both the surface of the flow cell and on surface of the particle. A particle can only bind when a binding site reacts with analyte and a free binding site on either surfaces. That means that the activity is 0 when all binding sites are free or all binding sites react with analyte. The activity is maximum when on the particle all binders react with analyte and all binders on the surface are free, and vice versa. The activity for the sandwich assay is given by

$$Activity \propto \theta_{particle} \cdot \left(1 - \theta_{surface}\right) + \left(1 - \theta_{particle}\right) \cdot \theta_{surface}. \tag{33}$$

A special situation occurs for $K_{d,particle} \vee K_{d,surface} = c_0$. For $K_d = c_0$ the fraction of free binding sites is $\frac{1}{2}$. The relative activity will then always be $\frac{1}{2}$ regardless of the fraction of free binding sites on the other surface.

The activity defined by equation 33 can be analyzed for different K_d's on the surface of the flow cell and the surface of the particle. In figure 2.3 the dependency of the activity on the K_d value on the surface of the flow cell, $K_{d,surface}$, and the K_d value on the particle, $K_{d,particle}$ is sketched. The axes are centered around $K_d = c_0$, with c_0 the analyte concentration. Five regions can be distinguished from figure 2.3. A relative activity of $\frac{1}{2}$ is found on the axes, region **V**, where the K_d value on either the surface of the flow cell or the surface of the particle is equal to the analyte concentration, c_0. In region **I** the relative activity will be less than $\frac{1}{2}$. For both surfaces $K_d > c_0$, the amount of free binding sites is larger than the fraction of reacting binders. The amount of combination of free and reacting binders is lower compared to the axes, hence $activity < \frac{1}{2}$. Analog for region **III** where for both surfaces $K_d < c_0$, the fraction of reacting binders is larger than the fraction of free binders. The amount of combination of free and reacting binders is lower than region **V** hence $activity < \frac{1}{2}$. For region **II** and **IV** the opposite is true. In region **II**

19

$K_{d,particle} < c_0$ but $K_{d,surface} > c_0$, this results in a higher fraction of free binders on the surface of the flow cell and lower fraction of free binding sites on the particle, compared to region **V**. The amount of combinations of free and reacting binding sites is larger, thus $activiy > \frac{1}{2}$. Similarly for region **IV**, where $K_{d,particle} > c_0$ but $K_{d,surface} < c_0$, the fraction of free binding sites is higher on the surface of the particle and the fraction of free biding sites is lower on the surface of the flow cell, than in region **V**, hence also here $activity > \frac{1}{2}$. The K_d's in BPM sandwich assays are chosen such that it operates in regions **I**, **II** and **V**.
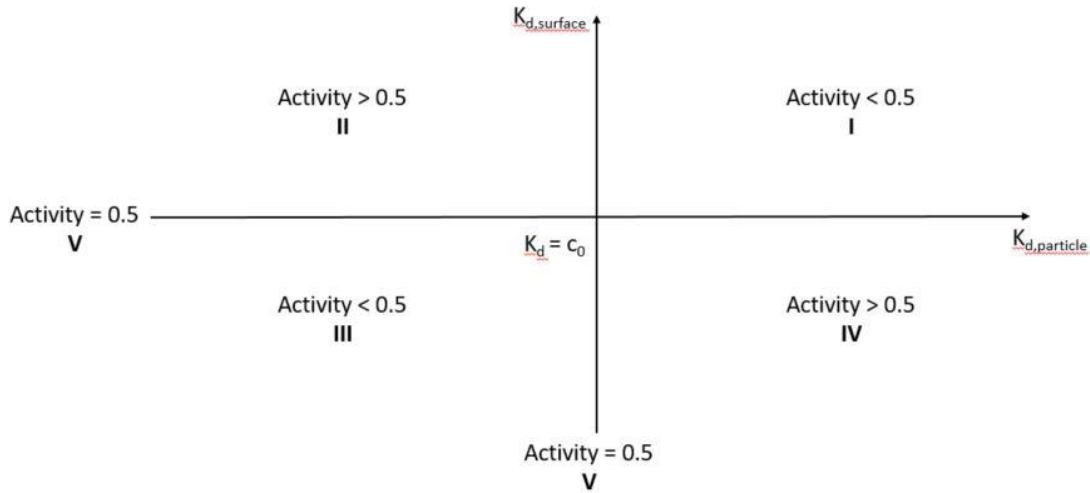

*Figure 2.3: A schematic sketch of the relative expected activity for BPM sandwich assays. The dissociation constant of the reaction on the particle, $K_{d,particle}$, is plotted on the horizontal axis, and $K_{d,surface}$, the dissociation constant of the reaction on the surface of the flow cell is plotted on the vertical axis. The axes are centered around $K_d = c_0$, with c_0 representing the analyte concentration of the sample. For $K_{d,particle} \vee K_{d,surface} = c_0$ the relative activity of the BPM sandwich assay is $\frac{1}{2}$, because the fraction of free binding sites is $\frac{1}{2}$ as well. This corresponds to region **V**. In region **I** the activiy is smaller than $\frac{1}{2}$, scine both K_d's are larger than c_0. This causes that both surface have an increased fraction of free binding sites relative to the axes, for which the combination of free and reacted binding sites is smaller than $\frac{1}{2}$. Analog for region **III** the activity is smaller than $\frac{1}{2}$ caused by the decreased fraction of free binding sites relative to the axes, which results in less combinatino of free and reacted binding sites. In contrast for regions **II** and **IV** where one K_d is larger and the other is smaller than c_0 the activity is larger than $\frac{1}{2}$, since the cominations of free and reacted binding sites is increased relative to the axes.*

20

3 INTRODUCING AND VALIDATING COMSOL

3.1 COMSOL

The activity measured with the BPM sensor depends on several physical processes; the transport of analyte by advection and diffusion, and the reaction of analyte with binders. There is no analytical solution neither for the time dependent analyte concentration nor the time dependent activity of the BPM sensor, when all processes are taken into consideration. The BPM sensor will be simulated to investigate the influence of advection, diffusion and reaction on the time dependent analyte concentration and the activity. COMSOL has been chosen for developing a model. COMSOL is a software package based om finite element methods (FEM) in which multiple scientific models can be combined into one simulation. [15]

Besides the ability to simulate multiple scientific models combined in one simulation, another advantage is to simulate the physical processes in the geometry of the BPM flow cell. This gives the opportunity to simulate the entire BPM sensor with taking into account the geometrical properties of the flow cell. Simulations can be performed for time dependent concentrations, different assay types and different values of k_{on}, k_{off} and K_d.

A disadvantage of COMSOL is that models might become computationally heavy. Simulating a large geometry with micro particles creates a locally fine mesh, by which the number of mesh elements increases. Consequently, few particles can be simulated before hitting the computational limit of the accessible equipment during this thesis. For computational convenience also the movement of the tethered micro particles has not been modelled.

3.2 VALIDATING COMSOL

In this section it will be investigated if COMSOL calculate physically correct results in the geometry of a BPM flow cell. With COMSOL flow, diffusion and surface reactions will be simulated. These three processes will be simulated and validated in test simulations. For validating flow and diffusion the BPM flow cell is simulated as a rigged channel with a rectangular cross-section of 5 mm × 250 μm. First the flow will be validated by comparing the simulated velocity profile with the analytical solution of the velocity profile presented in chapter 2 (equation 9), then diffusion of analyte will be validated by simulating a thin slice of concentration, as a delta peak, with a flowrate of zero and fitting the concentration profile with the solution of the diffusion equation, presented in chapter 2 (equation 18), for the initial condition of a delta peak and finally the reaction and implementation of reactive surface in COMSOL will be validated by reproducing a simulation performed by Squires et al.. [12]

Validating flow

To validate the velocity profile, the simulated flow velocities will be compared to the theoretical velocity profile from equation 9. A fluid flow with a flowrate of 30μL/min is simulated. The simulated velocity profile as a function of the height, h, at $y = 1/2w$ and as a function of the width, w, at $z = 1/2h$ are compared to the velocity profile from equation 9 in figures 3.1 and 3.2 respectively. The simulated velocity profile closely coincides with the theoretical velocity profile. It can be concluded that COMSOL will calculated the flow physically correct for the geometry of the BPM flow cell.
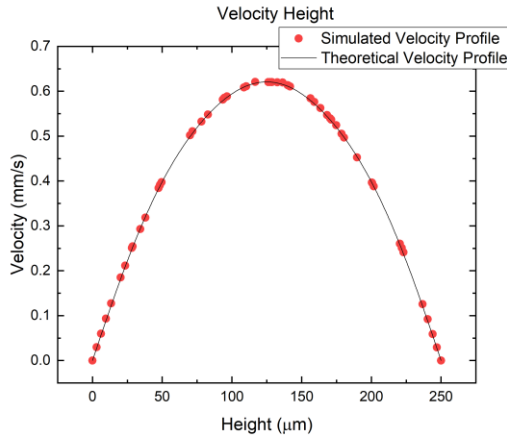
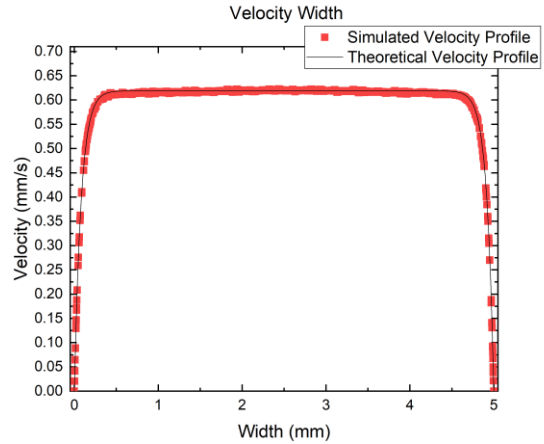| Figure 3.1: Simulated velocity profile in red for the height and theoretical velocity profile in black. The simulated velocity profile corresponds well to the theoretical profile. COMSOL is simulating the correct velocity profile for the height.	Figure 3.2: Simulated velocity profile in red for the width and the theoretical velocity profile in black. It can be seen that the simulated profile corresponds well with the theortical profile. COMSOL is simulating the correct velocity profile for the width.

Validating diffusion

For validating the diffusion of analyte molecules a thin slice of analyte concentration reaching in the width and the height of the flow cell with a thickness of 10µm will diffuse into the flow cell in the absence of a fluid flow. The analyte has a diffusion coefficient of 10^{-10} m²/s. The analyte molecules will only be able to diffuse over the length of the flow cell. The initial concentration profile as function of the length of the flow cell at $y = 1/2w$ and $z = 1/2h$ can be approximated as a delta peak. Equation 18 is solved for one dimension (only diffusion over the length, not the width or the height) with initial condition of a delta peak. This gives the following expression for the distribution of analyte, with diffusion coefficient, D, as function of the time, t, and the distance, x, from the initial location of the slice, x_0:

$$P(t,x) = \frac{1}{\sqrt{4\pi Dt}} e^{-\frac{(x-x_0)^2}{4Dt}}. \tag{34}$$

In figure 3.3 the simulated concentration profile after $t = 1000$ s is plotted. The data is fitted with equation 34. From the fit a diffusion coefficient of 10^{-10} m²/s was obtained, which corresponds with the diffusion coefficient used as input. This concludes that COMSOL will simulate the diffusion of analyte physically correct in the geometry of BPM sensor.
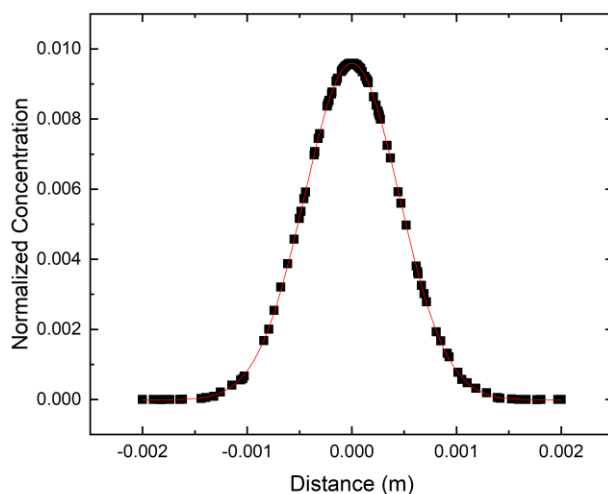
Figure 3.3: Concentration profile of a delta peak after 1000s. The data is fitted with equation 34. From the fit a diffusion coefficient of $10^{-10} m^2/s$ was calculated.

Reactions

Squires et al. (2008) have used COMSOL to simulate micro fluidic channels with surface reactions to study analyte depletion in flow. From the model of Squires the fraction of free binding sites can be calculated as well. The fraction of free binding site is needed to determine the activity of the BPM sensor. A modification of the model of Squires will be used to model the BPM sensor. In this section the model of Squires et al. (2008) will be reproduced, with the parameters used by Squires, to verify the implementation of the surface reaction that will be used in the model of the BPM sensor.

Squires has developed a 2D micro fluidic channel in which a microscale sensor is modeled as a flat square on the surface of the channel. The sensing surface is centered in the channel. Binders are attached to the sensing surface and the reaction between analyte and binders is affinity based. A sample with analyte is flown into the channel and analyte will react with the binders on the surface. The Damköhler number for this sensor is $Da \approx 3$. This implies that the time dependent development of the fraction of reacting bindings sites is neither dominated by transport nor reaction. The sensor reaches equilibrium on longer timescale than would be expected when the system would be model according to first order reaction kinetics. The simulation parameters are given in table 3.1.

Table 3.1: The simulation parameters used in the model of Squires et al. (2008).

Simulation parameter	
Channel length	100 μm
Channel width	100 μm
Channel height	100 μm
Sensor dimensions	50 μm×50 μm
Flow rate	10 μL/min
Analyte concentration	10 fM
Diffusion coefficient of the analyte molecules	$10^{-11} m^2/s$
k_{on}	$10^6 M^{-1}s^{-1}$
k_{off}	$10^{-3} s^{-1}$

K_d	10^{-9} M
Binding site areal density	$2 \cdot 10^{16}$ sites/m^2

In figure 3.4A the development of the dimensionless bound analyte (similar to the fraction of reacted binding sites) of the simulation performed by Squires, in which depletion of analyte is taken into account, is plotted in blue. The black graph shows development of the dimensionless bound analyte when the assumption is made that no depletion zone is formed. The time on which the dimensionless bound analyte develops is neither dominated by transport nor diffusion. This implies that the time constant on which equilibrium is reached is longer than the time constant based on first order reaction kinetics. In figure 3.4B the development of the dimensionless bound analyte is plotted of the recreated simulation. In figure 3.4C the results of the recreated simulation are plotted on top of the results from the model developed by Squires. The recreated simulated dimensionless bound analyte coincide with the dimensionless bound analyte simulated by Squires. This implies that the implementation, which is used to model reactions in the BPM sensor, is correct.
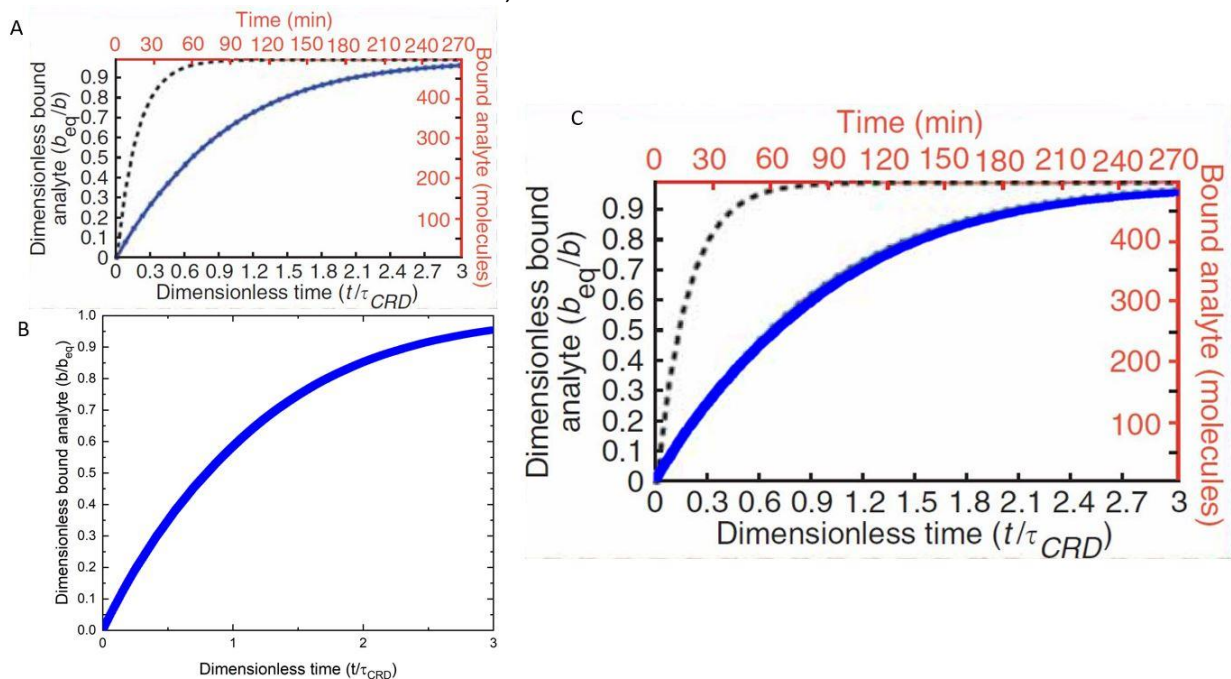

Figure 3.4: (A) The dimensionless bound analyte plotted as function of dimensionless time t/τ_{CRD}, with in black the depletion of analyte is not taken into account and in blue the depletion of analyte is taken into account. Figure retrieved from Todd M. Squires et al.. [12] Note that on the verticle axis an error was made, it should be (b/b_{eq}), the measured bound analyte over the amount of bound analyte in equilibrium, not (b_{eq}/b). (B) The simulated dimensionless bound analyte plotted as function of dimensionless time t/τ_{CRD} with the implementation of surface reaction as used for the simulations of the BPM sensor. (C) The simulated fraction of bound analyte by Squire(blue dotted line) s and the simulated fraction of bound analyte with the implementation of surface reaction as used in the simulations of the BPM sensor (blue solid line) plotted for dimensionless time t/τ_{CRD}. The simulated dimensionless bound analyte with the implementation of surface reaction as used in the simulation of the BPM sensor is in accordance with the dimensionless bound analyte simulated by Squires.

24

4 MODELING THE BPM SENSOR WITH COMSOL

For this project a 3D model of the BPM sensor is developed in COMSOL. Changing analyte concentration and the activity of the BPM sensor are simulated as function of time with including flow, diffusion and reaction of the analyte with binders on the particles and the surface. The model developed by Squires et al. (2008), verified in section 3.2, is modified to fit the dimensions of the BPM sensor. The 2D geometry of a micro fluidic channel is extended to a 3D geometry of the BPM flow cell. The reactive surface is extended to the entire bottom surface of the flow cell and a second surface reaction is added to the surface of the particles.

The assumptions and simplifications will be discussed in section 4.1, the model for the geometry of the flow cell will be discussed in section 4.2. The mesh is discussed in section 4.3. The simulation of flow, diffusion and reaction is discussed in section 4.4 and lastly the acquisition of results are discussed in section 4.5.

4.1 ASSUMPTIONS AND SIMPLIFICATIONS

In order to implement the geometry and operating conditions of the flow cell in COMSOL, several assumption and simplifications are made. In this section they will be listed and discussed.

For continuous monitoring with a BPM sensor the sample needs to be transported from the patient to the flow cell via a tube. For experiments tubes with typical lengths of 20-50 cm are used. The flow cell has a length of 3 cm which is small compared to the length of the tubes. Since the focus of thesis is on the distribution of time dependent analyte concentration in the flow cell and between particles and the surface, and since the length of the tubes vary between experiments and applications, it is chosen to simulate only a small part of the tube. The decision to simulate a small part of the tube and not to eliminate the tube from the geometry is to maintain and simulate the right inflow position of the sample in the flow cell. It will be assumed that the source of the sample directly connects to the tube. This implies that the concentration at $t = 0$ over the interface of the tube (where the fluid will flow into the geometry) is homogeneously spread. The influence of the tube length will be discussed in section 5.2.2.

The connection of the tube to the flow cell slightly differs for each experiment. In early flow cell designs, tubes are connected to pipet tips, which are glued under an angle to the flow cell. The connection of the tube to the flow cell is illustrated in figure 4.1. For recent flow cell design the tubes are connected to the flow cell by use of luer-lock connectors. For luer-lock connectors the tube is connected under a 90° angle. It has been chosen to model after recent flow cell designs. Thus the tube and the flow cell connect under an angle of 90°.

In early flow cell designs the tube is often connected with a distance to the backside of the flow cell as illustrated in figure 4.1. For recent flow cell designs the distance between the backside of the flow cell and the tube is minimized. For the geometry has been chosen to position the tube according to recent flow cell designs. The influence of the distance between the tube and the backside of the flow cell on the analyte concentration between the particle and the surface will be discussed in section 5.2.1.
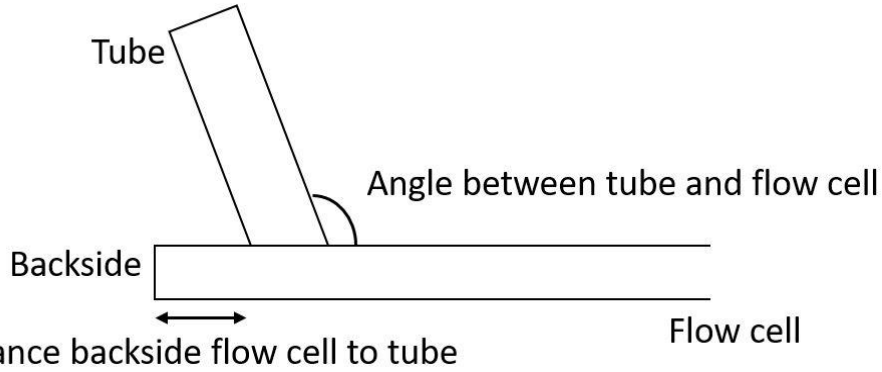
25

Figure 4.1: Schematic over view of the old flow cell design in which the tube is glued under an angle to the flow cell. In old flow cell designs a distance between the backside of the flow cell and the tube is present.

The BPM flow cell contains tether micro particles. The particle is assumed to be spherical and only one particle will be simulated instead of hundreds of particle to keep such that the simulation do not get computationally heavy. The tether is assumed rigged instead of flexible and it is assumed that the tether is much longer than thick and that it does not have an influence on the distribution of the analyte around the particle.

Even though the switching of particles is left out of the simulation (rigged tether), the fraction of free binding sites can be calculated on the surface of the particle and the flow cell. It is assumed that the fraction of free binding sites is representative for the activity of the BPM sensor and that all binding sites are able to react. It is possible that capture molecules are immobilized in such rotational position that they can no longer react with analyte. This will not change anything to the fraction of free binding sites, but this might cause that the BPM sensor reaches equilibrium on longer timescales.

4.2 GEOMETRY

A schematic top view of the geometry is shown in figure 4.2 and a side view is shown in figure 4.3. The flow cell has a height of 250μm and a total length of 30mm. The middle section of the geometry, the widest part of the flow cell, will be referred to as the main flow chamber of the BPM flow cell. At position A and B in figure 4.2, at the outside of the geometry, the tubes are connected to the flow cell at an angle of 90°. The tubes have a diameter of 0.56 mm and a length of 0.1 mm. Precisely in the center of the flow cell, at the red spot in figure 4.2, a micro particle with a radius of 500nm is positioned. The particle is positioned on a height of 75nm above the surface as schematically drawn in figure 4.4.
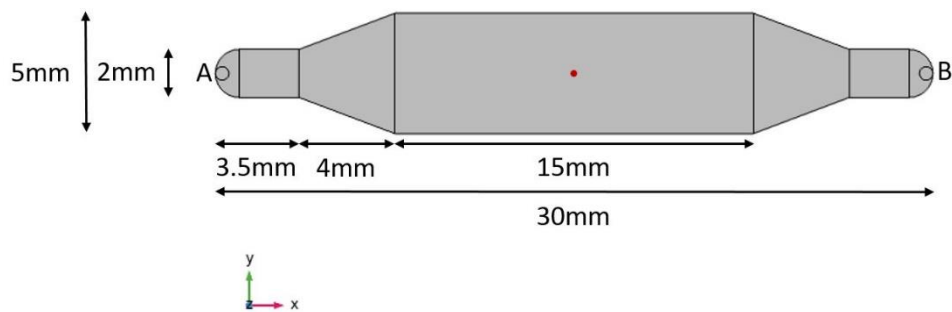

Figure 4.2: Top view and measurements of the modeled BPM flow cell. The height of the flow cell is 250μm. The tubes have radius of 0.28mm and a length of 0.1mm. On the red spot, in the center of the flow cell, a micro-particle with a radius of 500nm is placed.
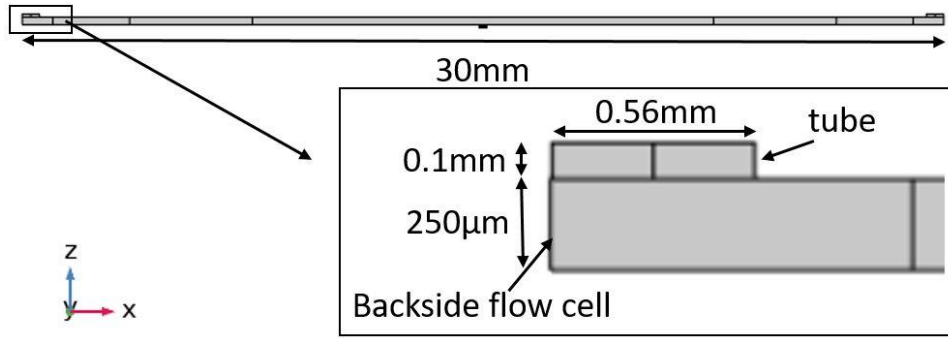
26

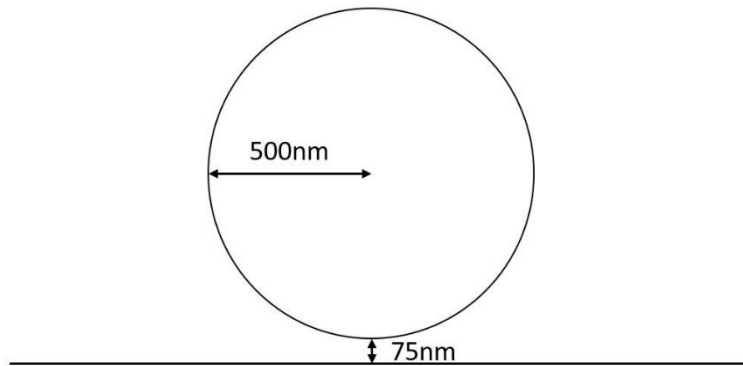Figure 4.3: Side view and close up of the flow cell and a tube.

Figure 4.4: A micro-particle with a radius of 500nm attached to the surface of the BPM flow cell with a tether of 75nm.

Some simulations have been performed in a reduced geometry, in which not the entire flow cell was simulated. The reduced geometry is shown in figure 4.5. The geometry is reduced to only one tube and the flow chamber is reduced to a length of 2mm. By reducing the geometry it was possible to make the model computationally lighter.
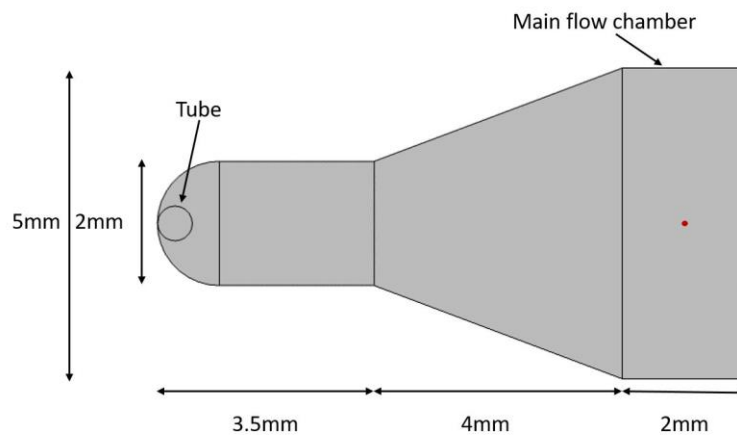

Figure 4.5: Reduced geometry of the BPM flow cell. It only contains the tube and the transistion of the tube to the main part of the flow cell, which is reduced to a length of 2mm. The tube has a length of 0.1mm and a diameter of 0.56mm.

27

4.3 Mesh

The geometry of the BPM flow cell is automatically meshed with tetrahedral elements by COMSOL. Free meshing, which is provided by COMSOL, was used to mesh the flow cell. Large mesh elements were used to mesh the flow cell, while fine mesh elements were used to mesh the particle and the region between the particle and the surface. The average quality of mesh elements is 0.6, with 1 being the best quality.

It is important to have a fine mesh at the surface of the flow cell. The analyte molecules will react with the surface of the flow cell and the particles. A concentration gradient is formed by the reaction, which is the depletion zone. To correctly simulated the depletion zone a fine mesh at the surface of the flow cell and at the surface of the particle is needed. The mesh in the bulk can remain coarse, since it is expected that due to stretching of the concentration gradient by shear flow, also known as Taylor dispersion.

4.4 Adding flow, diffusion of analyte and surface reaction

Flow

A laminar flow is simulated through the previously described geometry. In COMSOL the Laminar Flow module has been used. The sample flows through the top of the tube into the geometry with a flow rate of 30μL/min. The fluid in the flow cell have been chosen to be water, as well as the fluid carrying the analyte molecules. A no-slip boundary condition is applied to the walls of the flow cell and surface of the particle.

Diffusion

In order to simulate the diffusion of analyte molecules the Transport of Diluted Species module has been used. As described in the introduction the BPM sensor can be used to determine the concentration of biomarkers. An example of such biomarker is thrombin. Thrombin is an enzyme that has the main function of blood coagulation [22] and also plays a pivotal role in cancer growth. [16] Visser et al. (2018). has performed continuously measurements of bovine thrombin with the BPM sensor. Therefore it has been chosen to simulate for bovine thrombin. Bovine thrombin has a weight of 33.6kDa and a diffusion coefficient of $8.76 \cdot 10^{-11}$m^2/s at room temperature in water. [17] The concentration will be implemented as a step concentration as illustrated in figure 4.6. This the experimental situation in which a sample with a homogeneous analyte concentration is flow into the flow cell.
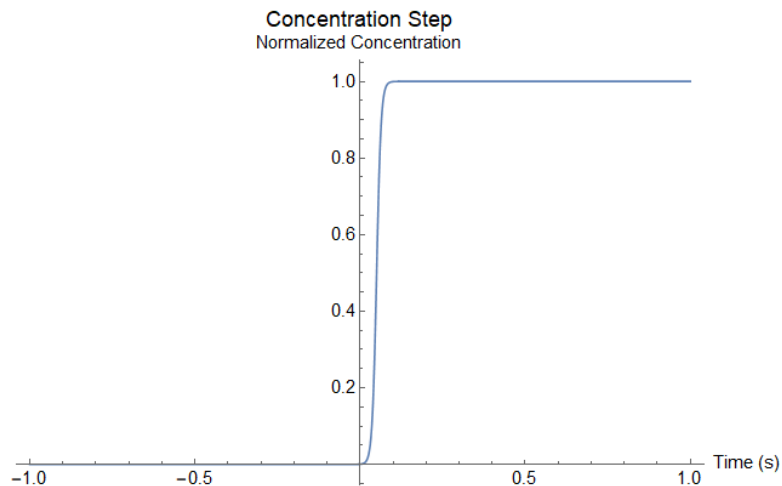
Figure 4.6: Step concentration implemented as time dependent increase of the analyte concentration.

Reaction

In order to simulate the response of the BPM sensor, the BPM competition assay and the BPM sandwich assay, which were introduced in sections 1.2, are implemented. The reaction between the binders and analyte is implemented with the COMSOL module Chemistry and Surface Reaction.

Competition assay

For implementing the competition assay, a reversible, affinity based reaction is simulated on the entire bottom surface of the flow cell. The binding site areal density on the surface of the BPM flow cell has been estimated to be 1 site/100nm², or 10^{16} sites/m². One analyte molecule can react with a single binder. The k_{on}, k_{off} and K_d parameters of the reaction will be given when the simulated results are discussed in section 5.4.

Sandwich assay

For implementing the sandwich assay, a second surface reaction is added to the model. On the surface of the micro particle an affinity based reaction is simulated as well. It has been estimated that there are 1 million binding sites present on a particle with a radius of 500 nm. This gives an binding site areal density of $3.18 \cdot 10^{17}$ sites/m². Also one analyte molecule can react with a single binder. The k_{on}, k_{off} and K_d parameters of the reaction on the particle as well as on the bottom surface of the flow cell are specified when the simulated results are discussed in section 5.5.

4.5   RESULTS

From the model the local analyte concentration but also the fraction of free binding sites on the bottom of the flow cell and the particle will be determined. In this section the locations where the parameters are calculated will be described.

Calculating analyte concentration and fraction of free binding sites

In figure 4.7 a schematic overview of the region under the particle is illustrated. The concentration is experimentally determined by the switching of particles between the bound and unbound state. Therefore the concentration between the particle and the surface will be calculated. The particle is

29

placed 75 nm above the surface, the analyte concentration is read out halfway between the particle and the surface on a height of 37.5 nm above the surface.

The activity is dependent on the fraction of free binding sites on the particle and on the surface of the flow cell. In figure 4.7 is indicated where the fraction of free binding sites will be calculated on the surface of the particle and the surface of the flow cell. Since the particle will bind with the surface, only the fraction of free binding sites on the bottom half of the particle has to be calculated. Yan et al. (2020) estimated that only 1% of the surface of the particle will be able to bind to the surface of the flow cell for a tether of 50 nm. This implies that only a fraction of the bottom hemisphere of the particle is reactive. The tether is located in the middle of the fraction of the surface of the particle that is able to react, therefore it is chosen to acquire the fraction of free binding sites at the tether position on the particle. The fraction of free binding sites on the surface is also read out at the position of the tether for the same reasons. Furthermore, the simulation results must be interpreted as an average result found for many performed experiments.
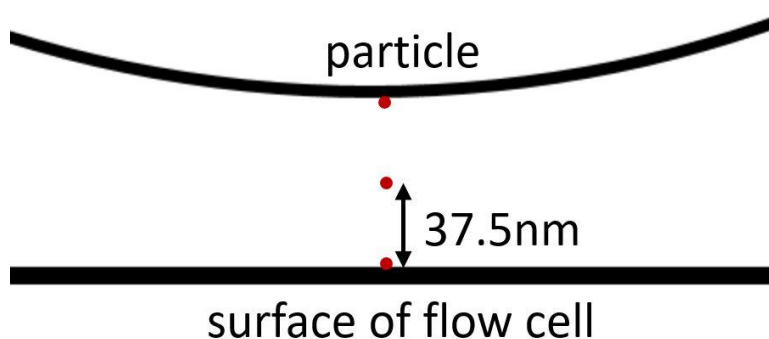

Figure 4.7: The time depedent analyte concentration will be calculated at 37.5 nm, close above the surface. This is at half tether length, or right in between the particle and surface of the flow cell. The fraction of free binding sites will be calculated at the location of indicated with a red dot on the surface of the particle and the flow cell.

Equilibrium

The BPM sensor has a statistical measurement error of 10%. Therefore the BPM sensor will be considered to have reached equilibrium when the time dependent analyte or activity stabilizes within 10% of the equilibrium value. The typically the BPM sensor can continuously measure analyte concentration over two orders of magnitude. When the analyte concentration or the activity is decreased to zero, the BPM sensor will be considered to be in equilibrium when the analyte concentration has dropped over 1% of the initial value.

5 RESULTS AND DISCUSSION

In this section the result of the COMSOL simulation will be discussed. In section 5.1-5.3 COMSOL simulation are performed to investigate the timescales of the transport of analyte by advection and diffusion through the flow cell. The transport of analyte to the surface and particle and the influence of particle will be discussed in section 5.1. The influence of the tube on the analyte concentration between a particle and the surface will be discussed in section 5.2. The development of a concentration pulse through the flow cell will be discussed in section 5.3. In section 5.4-5.5 COMSOL simulation will be discussed which are performed to investigate the influence of advection, diffusion and reactions on the timescale of the BPM response. The timescales for BPM competition assays will be discussed in section 5.4 and the timescales for BPM sandwich assays will be discussed in section 5.5.

5.1 TRANSPORT OF ANALYTE TO A MICRO-PARTICLE

Particles are an important part in the BPM flow cell. The concentration is determined by the binding and unbinding of particles on the substrate as discussed in section 1.2. Therefore it is important to investigate the concentration around particles. In this section the influence of the particles on the distribution of analyte close to the surface will be discussed as well as the timescale of the transport of analyte to the surface. The fluid flow around a micro-particle will be discussed by use of streamlines and vorticity.

The streamlines around a particle with a radius of 500nm are plotted in figure 5.1. The particle is placed 75 nm above the surface. The flow rate is 30 µL/min. Fluid elements, and thus also analyte transport by advection, takes place along the streamlines, as described in section 2.4. Figure 5.1 illustrates that there will be a fluid flow underneath the particle. This implies that analyte will be transported between the particle and the surface.
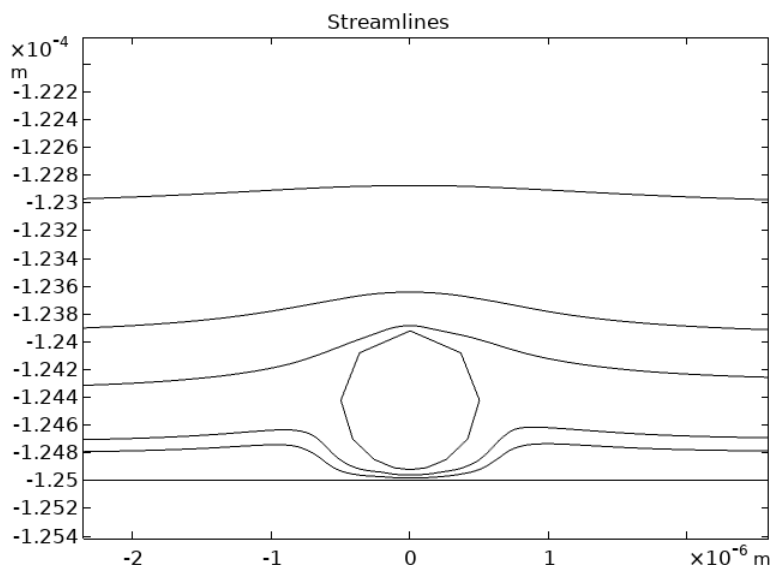

Figure 5.1: Side view of a particle with a radius of 500nm. Streamlines plotted around a micro-particle with a radii of $500nm$. The flow direction is from left to right. With the x-axis plotted horizontally and the z-axis plotted vertically.

Since the particle induces a change in the flow direction, it induces a change in vorticity as well. In figure 5.2 the y-component of the vorticity around a particle in the x,z-plane is plotted. Figure 5.2 illustrates that close to the particle the rotation of the fluid is strong compared to distances far away from the particle. The vorticity decreases as the distance to the particle increases. This implies that the influence of the particle has a finite range on the distribution of analyte in the fluid flow. The distance on which the influence of the particle in the fluid flow stretches can be determined by comparing the vorticity in the presence of the particle, with the vorticity in absence of the particle. In figure 5.3 the y-component of the vorticity in the x,z-plane in the absence of a particle is plotted. Comparing figure 5.2 and 5.3 shows that the particle induces a difference in vorticity 5 µm upstream and 5 µm downstream. When two particles are positioned on a distance closer than 5µm from each other, the distribution of the analyte between the particles will be influenced by both.
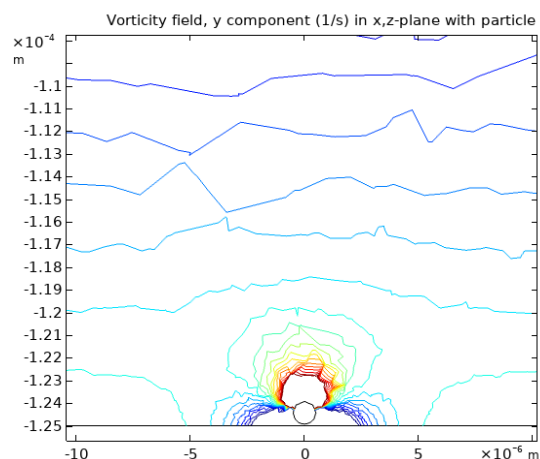

Figure 5.2: Vorticity plot of the y-component in the x,z-plane in the presence of a particle with a radius of 500nm. With the x-axis horizontally and the z-axis vertically. Flow direction from left to right.
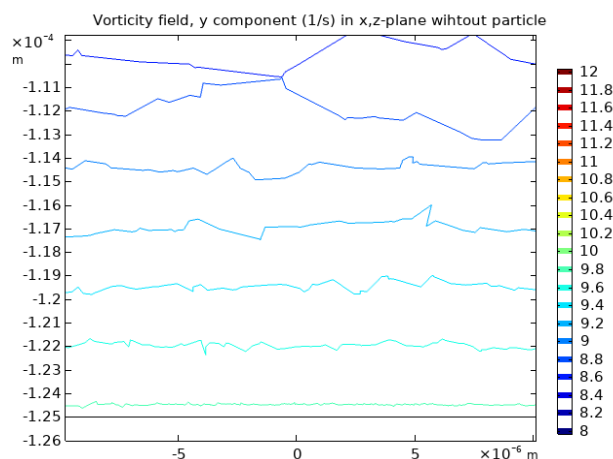
Figure 5.3: Voritcity plot of the y-component in the x,z-plane in the absence of a particle. With the x-axis horizontally and the z-axis vertically. Flow direction from left to right.

To investigate the influence of the particle on the analyte concentration close to the surface at 37.5 nm, a simulation with a particle and a simulation without a particle were performed. For both simulations the initial analyte concentration is zero. At $t = 0$ a sample with an analyte concentration of 1 nM enters the flow cell with a flowrate of 30 µL/min. The time dependent analyte concentration 37.5 nm above the surface in the presence and the absence of a particle is plotted in figure 5.4. Note that the tether length is 75 nm. The concentration is plotted normalized since the transport of analyte scales with the concentration gradient. See for more details Appendix A. The analyte concentration starts increasing at $t = 11$ s and reaches the analyte concentration of the sample within 10% at $t = 27$ s for both simulations. A minor difference in the development of the analyte concentration is visible at the start of the increase. This is caused by the influence of the particle on the fluid flow, and thus also on the analyte transport by advection. However, before 90% of the analyte concentration is reached, no difference is simulated in the increase of the analyte concentration. This implies that a particle does not have an influence on the timescale to increase the analyte concentration between the particle and the surface.
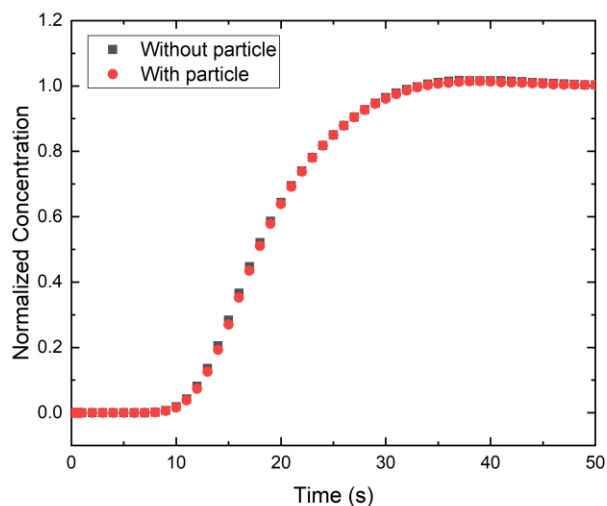
Figure 5.4: The analyte concentration measured 37.5nm above the surface for increasing concentration in absence of a particle, in black. The analyte cocnentration measured inbetween the particle and the surface on 37.5nm above the surface, in red.

To investigate why the particle does not have an influence on the timescale to increase the analyte concentration, simulation were carried out with transport by advection and diffusion, and with transport by only advection. Transport by only advection can be studied separately from transport by diffusion by eliminating the diffusion of analyte molecules, as described in section 2.4. For $D_{analyte} = 0$ m²/s a sample with an analyte concentration of 1nM enters the flow cell at $t = 0$. The development of the analyte concentration simulated between the particle and the surface for $D_{analyte} = 0$ m²/s is plotted in figure 5.5 together with the development of analyte concentration with diffusion. When the diffusion of the analyte molecules is eliminated the timescale for the analyte concentration to develop is increased from 25 s to 200 s. This implies that diffusion is dominant in the transport of analyte from the source to the region between a particle and the surface, since the timescales is increased from 25 s to 200 s.
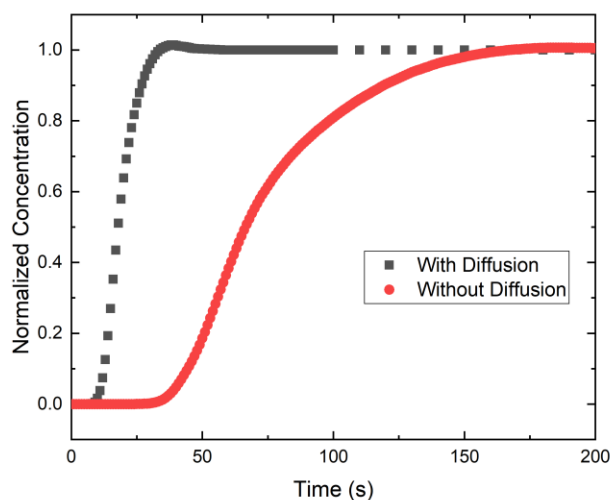
33

Figure 5.5: The time dependent analyte concentration between a particle of 500nm and the surface of the flow cell simulated with diffusion in black and without diffusion in red.

The dominance of diffusion on the distribution of the analyte concentration between the particle and the surface can be investigated by use of the Péclet number. In figure 5.6 the Péclet number is plotted for a characteristic length scale of 5 µm, which was determined to be the distance on which the particle has an influence on the fluid flow. Between the particle and the surface $Pe < 1$ which implies that diffusion is dominant in the distribution of analyte between the particle and the surface. The influence of the particle on the flow will has no significant influence on the distribution of analyte around the particle.
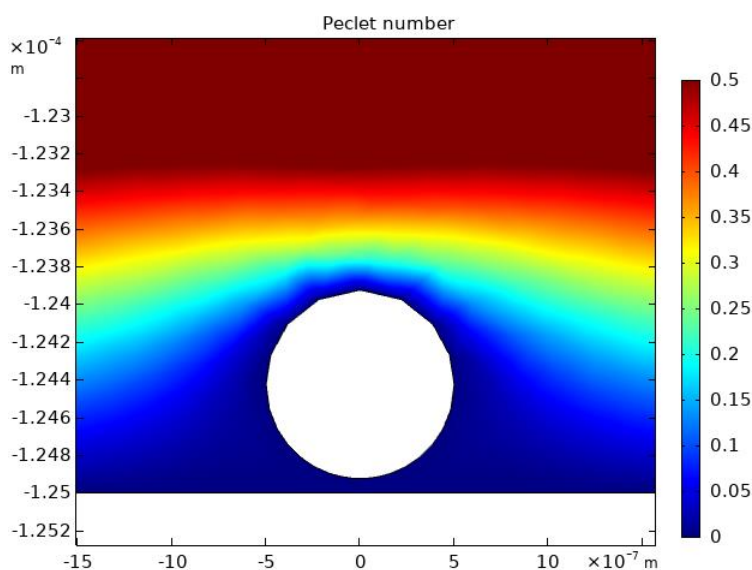

Figure 5.6: Péclet number around a particle with a radius of 500nm, for a characteristic length scale of 5µm. With the x-axis on horizontally and the z-axis vertically.

34

The simulations were carried out with a static tethered particle. However, in reality the tethered particle is moving by Brownian motion. In experiments the position of the particle in the flow will vary over the time. This implies that the influence of the particle on the fluid flow will vary over the time as well, and causes additional redistribution of the analyte concentration. Since diffusion is the dominant process in the transport of analyte around the particle, the analyte concentration of the sample will be reached between the particle and the surface regardless of the influence of the moving tethered particle on the fluid flow and thus also on the transport of analyte by advection.

In conclusion, the flow with and without a particle that has a fixed distance to the bottom of the flow cell representing a stiff tether, has been simulated. Fluid, and also analyte, will be transported by advection around, but more importantly underneath the particle. It was simulated that the presence of a particle does not have a significant influence on the timescale for increasing analyte concentration after introducing a sample, even though the particle has an influence on the fluid flow. This also has been illustrated by analyzing the Péclet number around the particle, for a typical length scale of 5μm, obtained from vorticity calculations. It was found that the transport of analyte around a particle is dominated by diffusion.

5.2 INFLUENCE OF THE TUBE ON THE TIME DEPENDENT ANALYTE CONCENTRATION

In this section, the influence of design parameters of the tube, that connects the patient and the flow cell, will be investigated. The influence of the design parameters on the timescale for decreasing and increasing analyte concentration will be discussed. In section 5.2.1 the influence of the placement of the tube is discussed and in section 5.2.2. the influence of the length of the tube will be discussed.

5.2.1 Tube placement

In early flow cell designs the tube is connected to the flow cell on a different position than the position of the tube in the recent design as shown in figure 4.2. In older designs the tube is placed more towards the main body of the flow cell and away from the curved backside of the flow cell as illustrated in figure 5.7. In this section the effect of the tube position relative to the end of the flow cell on the time dependent analyte concentration under a particle will be investigated.
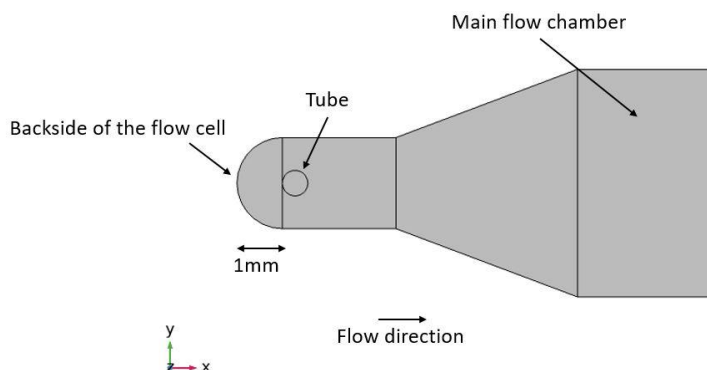

Figure 5.7: Close up of the flow cell on the region where the tube between the source and the flow cell is connected. The tube is placed 1 mm from the backside of the flow cell, which creates a region between the tube and the flow cell. The flow direction is from left to right, from the tube towards the main flow chamber.

The influence of the tube position will be investigated for decreasing analyte concentration. The initial analyte concentration in the flow cell is 1 mM. At $t = 0$ a fluid with no analyte molecules is flown into

the flow cell. The region between the tube and the backside of the flow cell will have an influence on the decrease of the analyte concentration between a particle and the surface, when the flow speeds in this region are low compared to the flow speeds in the region from the tube towards the flow cell. When the flow speed is low, the analyte concentration will remain higher in this region, while the concentration between the tube and the main flow chamber decreases faster due to the higher flow speeds. Since the molecules will need to be transported towards the main flow chamber, to be flown out of the flow cell, the analyte molecules might cause the analyte concentration between the particle and the surface to decrease on longer timescales.

To investigate the influence of the placement of the tube in early flow cell designs a fluid flow with a flowrate of 30 µL/min will be simulated in the geometry shown in figure 5.7. In figure 5.8 the flow speed is plotted at half the height of the flow cell. Note the flow cell has a height of 250 µm. The flow speeds between the tube and the backside of the flow cell appear to be lower compared to the flow speeds between the flow cell and the main flow chamber, even though the flow speeds between the tube and the main flow chamber vary as function of the position. This implies that transport by advection in the region between the tube and the backside of the flow cell is much slower than transport by advection from the tube to the main flow chamber.
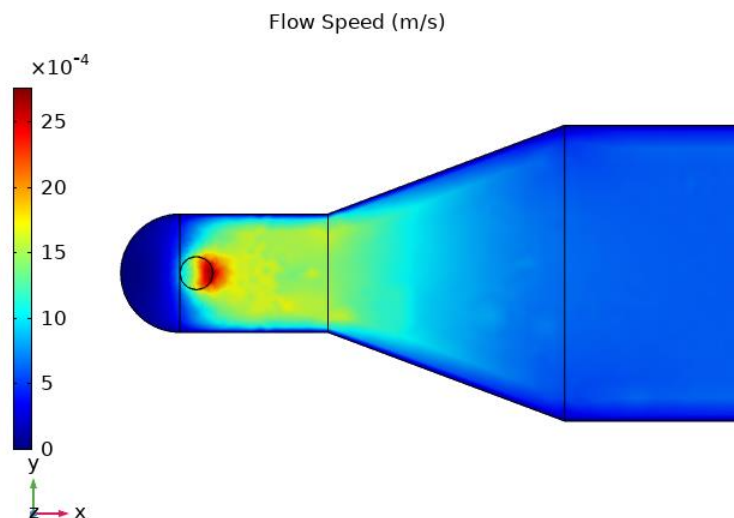

Figure 5.8: Flow speed (m/s) simulated for a flowrate of 30µL/min in the geometry seen in figure 5.7. The flow direction if from left to right.

To investigate what the effect of the difference in flow speed, caused by the placement of the tube, has on the time dependent analyte concentration between particles and the surface of the flow cell, COMSOL simulation will be carried out for different tube placements. A decrease of the analyte concentration to zero is simulated for different distances between the tube and the backside of the flow cell. At $t = 0$ a fluid is flown into the flow cell containing no analyte molecules. It is assumed that the analyte concentration is equal in the entire flow cell at $t = 0$. The decrease of the analyte concentration between particles and the surface for different distance between the tube and the backside of the flow cell are plotted in figure 5.9. A time of 70 s is required to decrease to 1% of the initial analyte concentration for three different tube positions. This implies that the simulated time required to decrease to 1% of the initial analyte concentration is unaffected by the position of the tube.

A small difference can be seen between the time dependent analyte concentration in figure 5.9. For a distance of 1.72 mm between the tube and the backside of the flow cell it can be seen that the time required to decrease the analyte concentration is a second shorter than for a distance of 0 mm. A distance of 1.72 mm from the backside of the flow cell means that the tube is positioned 1.72 mm closer to the main flow chamber. This implies that the fluid without analyte molecules is flown over 1.72 mm flow cell less compared to a distance between the backside and the tube of zero.
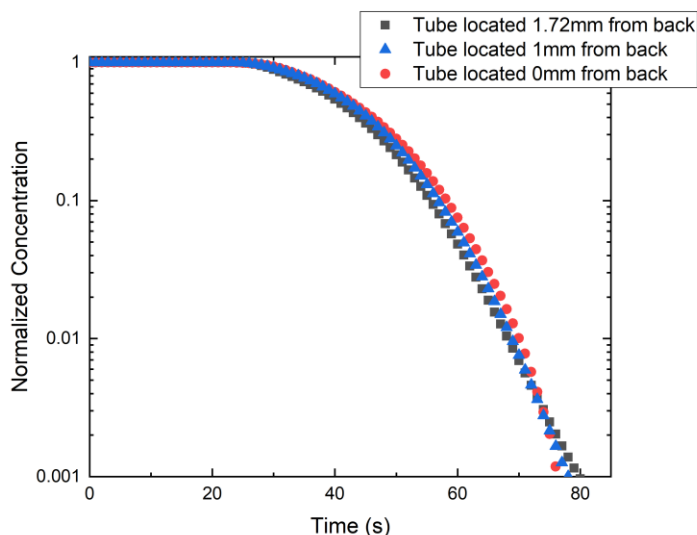

Figure 5.9: Development of decreasing analyte concentration between a particle and the surface of the flow cell for different distance between the tube and the backside of the flow cell of 0mm, 1mm and 1.72mm. For longer distances between the tube and the back side of the flow cell, the analyte concentration decreases slower after two orders of magnitude.

Visser et al. (2018) have performed experiments in BPM sandwich assays in which the analyte concentration in the BPM flow cell was decreased to zero by flowing in a fluid with no analyte molecules. It was determined that the timescale to decrease the activity to zero is in the order of hours. Since the activity of the BPM sensor is dependent on the analyte concentration between particles and the surface, the timescale to decrease the analyte concentration is in the same order. Since the placement of the tubes does not cause the analyte concentration between particles and the surface to decrease on a timescale in the order of hours, but rather minutes, the placement of the tube does not influence the analyte concentration between particles and the surface.

5.2.2   Tube length

In section 4.1 it was mentioned that tubes with typical lengths of 20-50 cm between the patient and the flow cell are used. Obviously, the distance between the patient and the flow cell, over which the analyte has to be transported, is dependent on the length of the tube. In order to investigate the influence of the tube length on the analyte concentration between a particle and the surface, simulation have been carried out. The geometry used for the COMSOL simulation contains a tube with a length of either 0.1 mm or 150 mm and the time dependent analyte concentration between a particle and the surface will be investigated.

The initial analyte concentration in the flow cell and the tube is 0 M. At $t = 0$ a sample will enter the tube with an analyte concentration 1 mM at a flowrate of 30 µL/min. In figure 5.10 the anlatye

37

concentration is plotted against the time between a particle and the surface of the flow cell. For the tube of 0.1 mm the analyte concentration start increasing at $t = 13$ s and reaches 90% of the sample's analyte concentration after $t = 29$ s. For the tube of 150 mm, the analyte concentration starts increasing at $t = 63$ s and reaches 90% of the sample's analyte concentration after t=119 s. It takes 70 s longer for the analyte concentration to increase. Obviously this difference is caused by the difference in the tube lengths. When more time is required to increase the analyte concentration, the concentration profile is stretched over a longer distance. This decreases the concentration gradient. This implies that the concentration difference measured over a distance, e.g. a field of view, decreases for longer tubes.

From the time difference between the tubes it can be determined if the simulation is calculating physically correct times. It takes 50 s for the front of the concentration profile to be transported over a tube of 150 mm. The concentration front is carried by the flow, but due to the shear flow and a high Péclet number of $6.5 \cdot 10^3$ it will be stretched along the flow direction enhancing the rate the concentration is transported along the flow. This effect is named Taylor dispersion. The concentration profile will be stretched over in the radial direction of the tube as well. Besides the displacement of the concentration profile by the flow, the profile will disperse. For a flowrate of 30 µL/min, tube radius of 0.28 mm and a diffusion coefficient of $8.76 \cdot 10^{-11}$ m²/s a dispersion coefficient of $8.7 \cdot 10^{-7}$ m²/s is found. [19] [20] This causes the concentration profile to be dispersed over 5 cm after 50 s. This implies that the concentration profile is effectively carried over 10 cm by the flow. The average flow velocity in the tube is 2 mm/s and thus it takes 50 s to flow over the effective 10 cm. This implies that the simulation is carried out well.
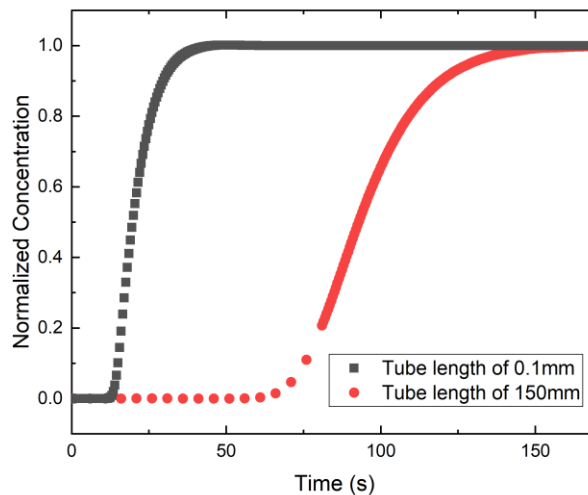

Figure 5.10: The development of the analyte concentration between a particle and the surface for a tube of 0.1mm in black and a tube of 150mm in red.

To investigate if the dispersion in the concentration profile is not caused by the mesh two simulation were carried out meshed with more an less mesh elements as for the simulation in figure 5.10. In figure 5.11 the time dependent analyte concentration at 140mm downstream in the center tube is plotted. The 150 mm tube used in the previous simulation of figure 5.10 is meshed with $125 \cdot 10^3$ mesh elements. Figure 5.11 shows that the simulation from figure 5.10 has calculated the same concentration profile as for the simulations with $240 \cdot 10^3$ mesh elements. This implies that the tube from in the

38

COMSOL simulation from figure 5.10 is meshed with a sufficient number of mesh elements and that the stretching of the concentration profile is not caused by an insufficient mesh.
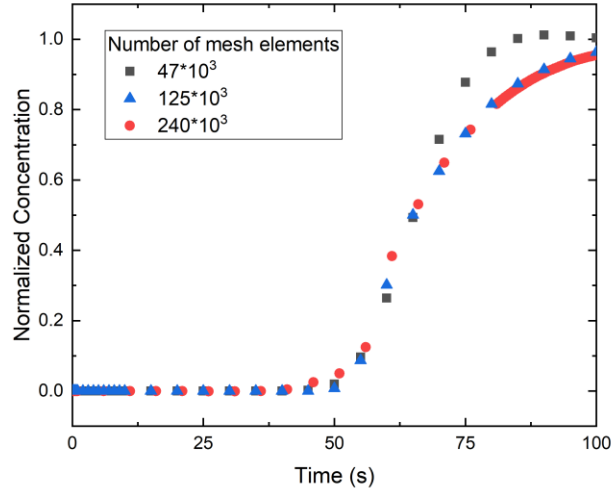

Figure 5.11: Time dependent analyte concentration at 140 mm downstream in the center of the tube plotted for different amounts of mesh elements used to mesh the tube.

5.3 THE DEVELOPMENT OF A CONCENTRATION PULSE IN THE BPM FLOW CELL

During continuous monitoring the analyte concentration of the sample might be increased for a short period of time before decreasing back to the initial analyte concentration. A block pulse of analyte concentration will be distributed through the flow cell by advection and diffusion and has been investigated with COMSOL simulations. A concentration pulse as shown in figure 5.12 is simulated in the geometry of figure 5.14. The initial analyte concentration in the flow cell is 0 M and a fully developed laminar flow is present in the flow cell.
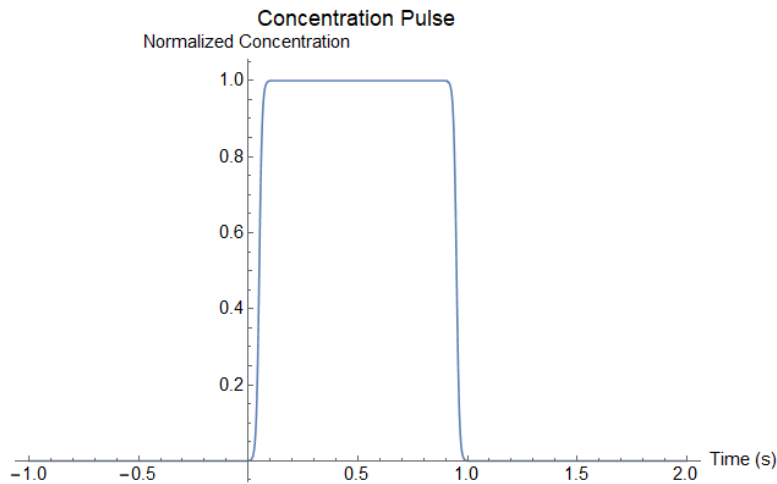

Figure 5.12: Block concentration pulse with a width of 1s.

The normalized analyte concentration is plotted as a function of time in figure 5.13 for the positions shown in figure 5.14 at 37.5 nm above the surface. The maximum calculated analyte concentration is lower than the analyte concentration of the pulse. This is caused by the broadening of the pulse by Taylor dispersion. Due to the shear flow the concentration profile disperses in the flow direction. This causes that the pulse to stretch in the flow direction and to be wider than the initial pulse length of 1 s. Since the amount of analyte molecules in the pulse must be conserved, the maximum simulated analyte concentration is lower than the initial concentration of the pulse.
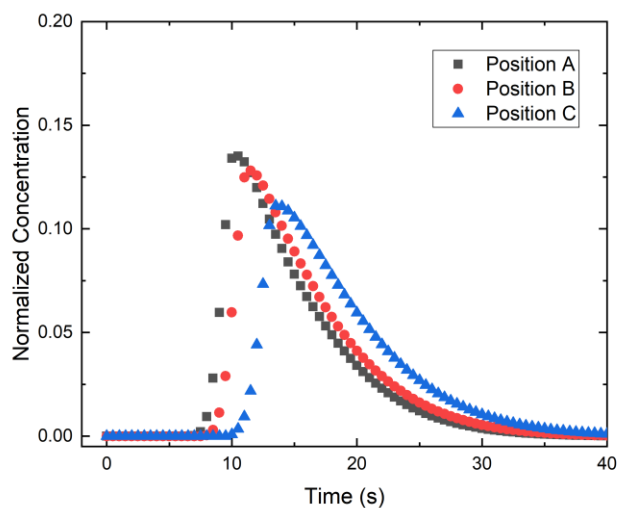

Figure 5.13: Development of the analyte concentration 37.5 nm above the surface for a concentration pulse of 1s. The measurement location are shown in figure 5.14.
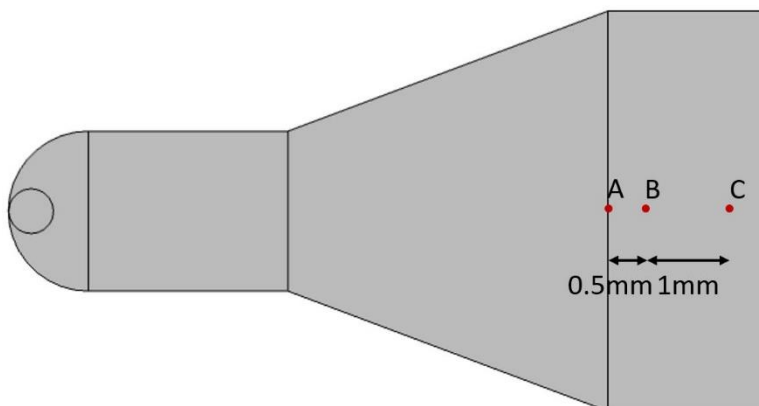

Figure 5.14: Measurement location for the concentration pulse at a height of 37.5 nm above the surface of the flow cell.

The concentration profiles plotted in figure 5.13 are increasing on a short time of 5s, but are decreasing on a longer time of 25s. To investigate why the time required to decrease is longer than the time required to increase a simulation was carried out in which the diffusion of analyte is eliminated. In figure 5.15 the analyte concentration is plotted as function of the width of the flow cell after 10 and 12 s simulated with diffusion and after 12 s simulated without diffusion on a height of 125µm above the surface. Due to the difference in flow speed in the width, the top of the pulse arrives earlier in the middle of the flow cell, than at the side walls of the flow cell. By comparing the simulation at $t = 12$ s

with and without diffusion it can be seen that the concentration at the walls is higher for the simulation without diffusion, but the concentration in the center of the flow cell is lower compared to the simulation with diffusion. This implies that analyte molecules are diffusing from the walls to the center of the flow cell. Thus the time required for the concentration to decrease is extended due to the diffusion of analyte from the walls of the flow cell (width) to the center.
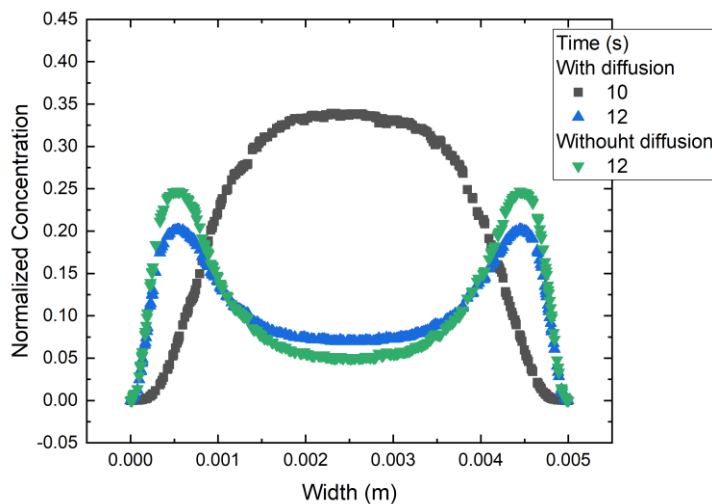

Figure 5.15: The distribution of a 1s block pulse in the BPM flow cell as function of the width at a height of 125µm above the surface after 10 and 12 seconds simulated with diffusion in black and blue respectively and after 12 seconds simulated without diffusion in green.

Summarized, the maximum simulated concentration at a height of 37.5nm is lower compared to the initial concentration of the pulse. This is caused by the dispersion of the concentration pofile. The time required to increase the analyte concentration profile is 5s, which is shorter the time required to decrease of 25s. Due to the diffusion of analyte from the wall to the center of the flow cell the time required for the analyte concentration to decrease is extended.

5.4 BPM COMPETITION ASSAY

Simulations performed for the BPM competition assay, introduced in section 1.2.1, will be discussed in this section. As described in section 4.4, at the bottom surface of the flow cell, binders are attached, with which analyte can react. The development of the time dependent analyte concentration and formation of a depletion zone will be discussed. Furthermore the influence of k_{on}, k_{off} and K_d on the local analyte concentration, the activity of the assay and the time to reach equilibrium for an increasing analyte concentration will be discussed in section 5.4.1. The influence of k_d, k_{off} and K_d on the local analyte concentration, the activity of the assay and the time to reach a concentration of zero for a decreasing concentration will be discussed in section 5.4.2.

5.4.1   Influence of reactions on the increase of analyte concentration and the BPM response

In this section the influence of the reaction parameters k_{on}, k_{off} and K_d on the increase of the analyte concentration, the relative activity, based on the fraction of free binding sites, and the time to reach the analyte concentration of the sample will be discussed. The flow cell has an initial concentration of 0 M

41

and at $t = 0$ a sample with an analyte concentration of 1 nM, implemented as a step concentration, flows into the flow cell.

Figure 5.16 shows the time dependent analyte concentration above the reactive surface of a BPM competition assay in green, in black the distribution of the analyte concentration above a non-reactive surface, and the fraction of free binding sites in blue. The initial analyte concentration is 0M. The analyte concentration starts increasing at $t = 11$s. After $t = 680$ s the concentration stabilizes at the 10% of the analyte concentration of the sample and the fraction of free binding sites reaches equilibrium at 0.99. The relative activity, as defined by equation 32, is 0.99 as well. The analyte concentration increases in two phases. During phase 1, as shown in orange area figure 5.16, the sample is distributed over the flow cell and between the particles and the surface of the flow cell. Analyte from the sample reacts with binders at the surface during phase 1. The reaction causes the analyte concentration to be lower compared to the analyte concentration above a non-reactive surface. In phase 1 the dominant process is the distribution of the analyte by advection and diffusion. The reaction of analyte with binders causes a concentration gradient towards the surface. This will be discussed later in this section.

The reaction is dominant in phase 2, purple in figure 5.16. Since the sample has been distributed between the particles and the surface during phase 1 and fresh sample is still transported through the geometry, the local analyte concentration will increase and the depletion zone will disappear. In equilibrium the number of reacted binders is constant and thus the amount of analyte that reacts with binders and the amount of analyte that unbinds is in equilibrium. Eventually the local analyte concentration will stabilize at the analyte concentration of the sample.
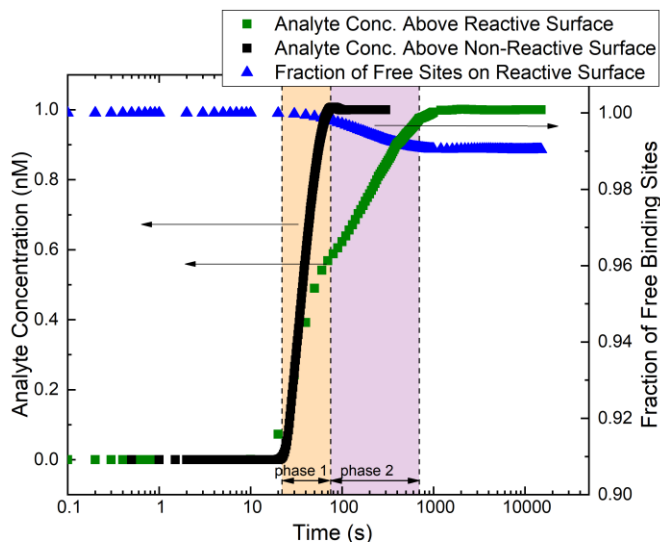

Figure 5.16: The development of the analyte concentration at 37.5 nm above the surface of the BPM flow cell for BPM competition assay, in green. In black the distribution of the sample above a non-reactive surface and in blue the development of the fraction of free binding sites at the surface. The reaction parameters used in the simulation were $k_{on} = 10^5 M^{-1}s^{-1}$, $k_{off} = 10^{-2}s^{-1}$ and $K_d = 10^{-7}M$.

The Damköhler number for the used assay is 1.5, which implies that neither the transport of analyte nor the reaction is dominant. In figure 2.2 it can determined that the timescale to reach equilibrium is $\tau_{CRD} = 3 \cdot \tau_r$. For this simulation $\tau_r = 99$s, so $\tau_{CRD} = 297$s. Note that τ_{CRD} is an exponential time

42

constant. The time at which 90% of the analyte concentration of the sample is reached and the fraction of free binding site reaches equilibrium corresponds with a time of 680 s.

Two additional simulations are performed, that are variations on the simulation shown in figure 5.16. By varying the reaction parameters, the influence of the reaction parameters on the time dependent response of the BPM flow cell can be investigated. Varying either the k_{on} or the k_{off} parameter will automatically causes the K_d parameter to be varied as well. Therefore, the variations of k_{on} and k_{off} are chosen such that K_d is unchanged. For one simulation k_{on} is increased by one order of magnitude, from 10^5 M^{-1}s^{-1} to 10^6 M^{-1}s^{-1}, for the other simulation the k_{off} is decreased by one order of magnitude, from 10^{-2} s^{-1} to 10^{-3} s^{-1}, such that for both simulations $K_d = 10^{-8}M$. For all simulation at $t = 0$ a sample is flown into the flow cell with an analyte concentration of 1 nM. The initial analyte concentration in the flow cell is 0 M.

In figure 5.17 the relative BPM activity and the fraction of free binding sites are plotted for $K_d = 10^{-7}$ M and 10^{-8} M. For equal K_d an equal BPM activity and fraction of free binding sites is found. The BPM activity in equilibrium is independent of k_{on} and k_{off} for equal K_d. The value for the K_d parameter determines the fraction of free binding sites in equilibrium for equal analyte concentration. In section 2.8 it was derived that the activity reduces for decreasing fractions of free binding sites.
The time required to reach equilibrium is indicated in figure 5.17. The time required to reach equilibrium for $K_d = 10^{-7}$ M is 680 s which is shorter than the 4400 s and 7600 s for the simulations of $K_d = 10^{-8}$ M. For lower K_d the fraction of free binding sites in equilibrium decreases, thus more binders will react with analyte in equilibrium. More analyte is required near the surface to reach equilibrium. Therefore the time to reach equilibrium in the BPM flow cell increases for decreasing K_d.
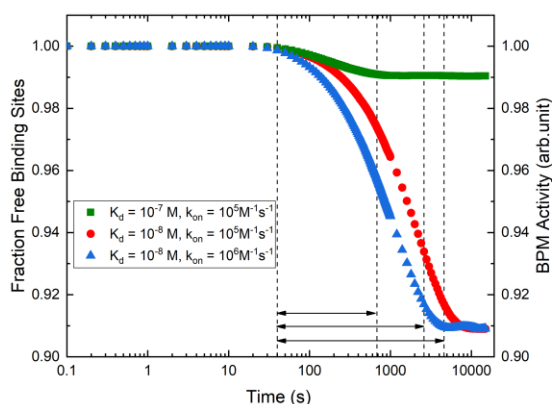

Figure 5.17: The time dependent fraction of free binding sites and relative BPM activity for different reaction parameters.
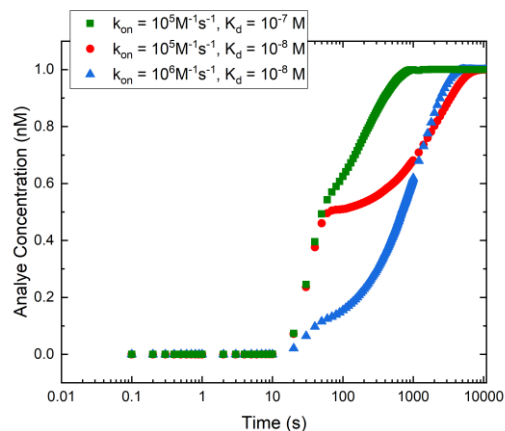

Figure 5.18: The time dependent analyte concentration close to the surface for different reaction parameters.

In figure 5.18 the development of the concentration is plotted for different k_{on}, k_{off} and K_d values. The k_{on} parameter has an influence on phase 1 of the development of the concentration. The size of the depletion zone is specific for one value of k_{on}. For higher k_{on} values the depletion zone is larger in size. This is illustrated in figures 5.19. For higher k_{on} more analyte binds per unit of time. Consequently the local analyte concentration is lower for higher k_{on}, since more analyte is taken out the sample by the

reaction. This induces a stronger concentration gradient towards the surface, which causes a larger depletion zone. However, the depletion zone has a maximum size for sufficiently high k_{on}. The limiting case in which the k_{on} is sufficiently high such that all analyte molecules bind to the surface is discussed in section 2.6.
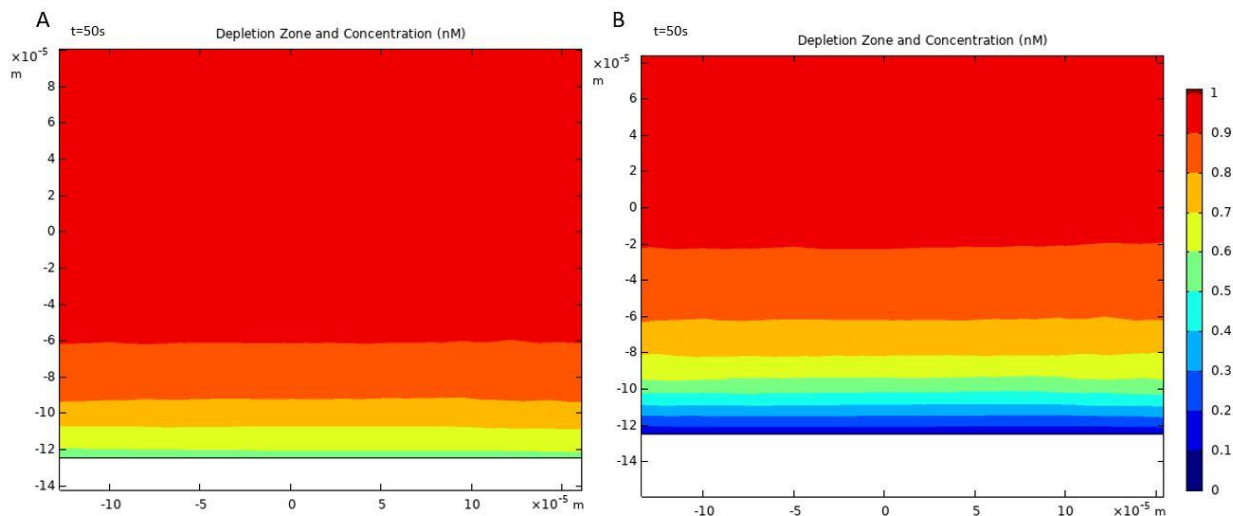

Figure 5.19: Depletion zone in BPM competition assay after 50s for $k_{on} = 10^5 M^{-1}s^{-1}$ in A and $k_{on} = 10^6 M^{-1}s^{-1}$ in B. No particles are present in the flow cell. The concentration (nM) is plotted in the x,z-plane with the x-axis horizontally and z-axis vertically with 0 the center of the main flow chamber. The legend on the rigth holds for A as well as for B.

From figure 5.17 it can be concluded that for equal K_d equilibrium is reached faster for a higher k_{on} value. For $K_d = 10^{-8}$ M and $k_{on} = 10^5$ M^{-1}s^{-1} equilibrium is reached after $t = 7600$ s and for $K_d = 10^{-8}$ M and $k_{on} = 10^6$ M^{-1}s^{-1} equilibrium is reached after t = 4400 s. So for higher k_{on} more analyte molecules binds per unit of time and the equilibrium is reached faster. However there is a critical k_{on} value for which the time does not decrease further. When the time at which the BPM activity reaches equilibrium is limited by transport, Da $\gg 1$, the time to reach equilibrium, τ_{CDR}, is independent of k_{on}. For lower Damköhler numbers the times is not proportional with k_{on}. For $k_{on} = 10^6$ M^{-1}s^{-1} equilibrium is reached twice as fast than for $k_{on} = 10^5$ M^{-1}s^{-1}. The corresponding Damköhler numbers are ~15 and ~1.5 respectively. From figure 2.2 it can be determined that for $k_{on} = 10^5$M $^{-1}$s^{-1} the timescale to reach equilibrium $\tau_r Da$ is twice as long as for $k_{on} = 10^6$ M^{-1}s^{-1}.

5.4.2   Influence of reaction on the decrease of analyte concentration and the BPM response

In this section the influence of the reaction parameters k_{on}, k_{off} and K_d as well as the influence of the initial analyte concentration on the time dependent decrease of the analyte concentration to zero and the relative activity will be discussed. The same analysis as in section 5.4.1 is performed for time dependent decreasing analyte concentration to zero. The analyte concentration at $t = 0$ is 1 nM. At $t = 0$ a fluid with no analyte molecules is flown into the flow cell.

In figure 5.20 the decrease of the local analyte concentration is plotted as a function of time. At $t = 0$ the analyte concentration is 1nM and will decrease at $t = 11$ s. After $t = 5 \cdot 10^4$ s the analyte concentration has decreased over 3 orders of magnitude. Similarly as for increasing analyte concentration for decreasing analyte concentration, the decrease occurs in two phases. During phase 1 the decrease is dominated by the transport of the analyte out of the flow cell. During this phase, the

44

analyte concentration under a particle decreases to 37% of the initial analyte concentration. During phase 2 the decrease in concentration is dominated by the dissociation of analyte molecules and binders. The timescale for decreasing the analyte concentration should be in the order of $\frac{1}{k_{off}} = 10^4$ s, but a longer time of $5 \cdot 10^4$ s is simulated for the decrease of the analyte concentration under a particle. A decrease of $5 \cdot 10^4$ s corresponds with 833 min. Unbound analyte molecules will be transported out of the flow cell. Analyte molecules that have dissociated from binders upstream, will contribute to the analyte concentrations downstream. Analyte molecules that are transported downstream can react again with binders, which will increase the timescale on which the analyte concentration decreases to 0.
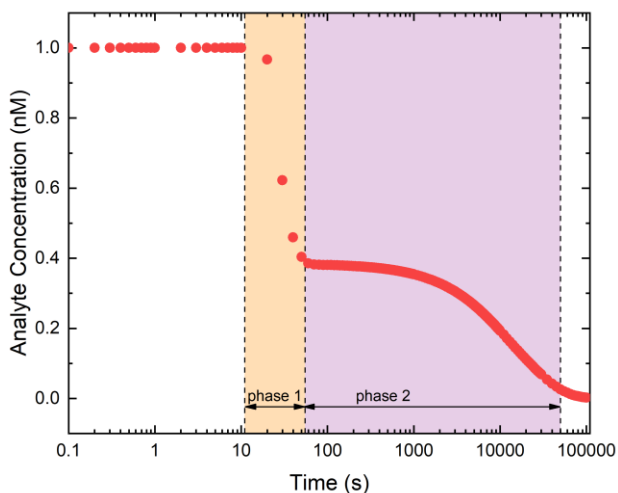

Figure 5.20: Development for decreasing analyte concentration in BPM competition assay.Simulated for reaction parameters: $K_d = 10^{-9}$ M, $k_{on} = 10^5$ M^{-1}s^{-1} and $k_{off} = 10^{-4}$ s^{-1}.

Two additional simulations are performed, that are variations on the simulation shown in figure 5.20. The variations of k_{on} and K_d are chosen such that k_{off} is unchanged. At $t = 0$ the concentration in the flow cell is 1nM. The reaction on the surface is in equilibrium. At $t = 0$ a fluid with no analyte molecules is flown into the geometry.
In figure 5.21 the decrease of the analyte concentration is plotted for both simulations and for the simulation of the previous section. For larger k_{off} the local analyte concentration remains higher than for lower k_{off}. For higher k_{off} analyte dissociates faster from binders and more analyte is diffusing back into the fluid. In figure 5.22 the decrease of the relative activity is plotted for both simulations. For equal K_d equal activity in equilibrium is found. The timescale to decrease the analyte concentration to zero is increased for lower K_d, since more analyte molecules are reacted with binders in equilibrium and thus more analyte molecules need to dissociate with binders. For $k_{off} = 10^{-4}$ s^{-1} and $K_d = 10^{-9}$ M the response time is $5 \cdot 10^4$ s. For $k_{off} = 10^{-3}$ s^{-1} and $K_d = 10^{-9}$ M the response time is 26000 s and for $k_{off} = 10^{-3}$ s^{-1} and $K_d = 10^{-8}$ M the response time is 4400 s. The simulated time response for $k_{off} = 10^{-3}$s^{-1} and $K_d = 10^{-8}$M is in the same order as the measured experimental time response of 120min (7200s). This implies that the measured experimental timescale, measured by Visser et al. (2018), is most likely caused by the rebinding of analyte molecules which have previously dissociated with binders on the surface upstream in the flow cell.
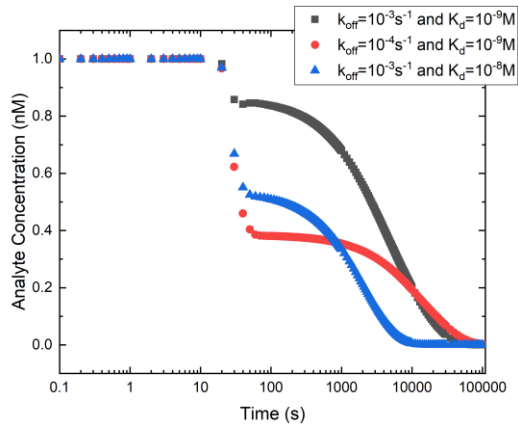
45

Figure 5.21: Development of decreasing analyte concentration close to the surface for BPM competition assay.
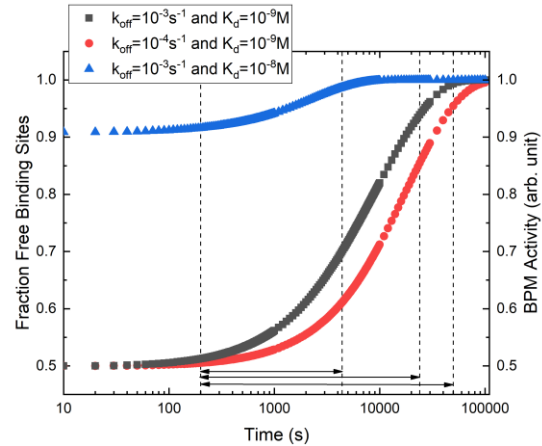

Figure 5.22: Development of the fraction of free binding sites for BPM compeition assay, when reversing the sensor.

With a BPM competition assay a range of different analyte concentration can be measured. In this paragraph for one set of reaction parameters, two simulation are performed for two different analyte concentrations of 1nM and 10 nM. At $t = 0$ the analyte concentration in the BPM flow cell is either 1 nM or 10 nM and a fluid without analyte molecules is flow into the geometry. The reaction is in equilibrium, but the activity in equilibrium is different depending on the analyte concentration as can be seen from figure 5.23. In figure 5.23 the increase of the activity and the increase of the fraction of free binding sites as a function of time is plotted for both simulations. Even though in equilibrium more analyte is bound to the surface for an analyte concentration of 10 nM than for 1 nM, the time to decrease the activity by 90% is 4400s for both concentrations. The time required to increase the activity to relatively 1 is independent of the initial analyte concentration in the flow cell. Yan et al. (2020) have performed continuous measurements in BPM competition assay in the nM regime. They decreased the analyte concentration to zero after increasing the analyte concentration. This was performed for several increases to different analyte concentration. No time differences were measured between the decreases from different analyte concentrations.
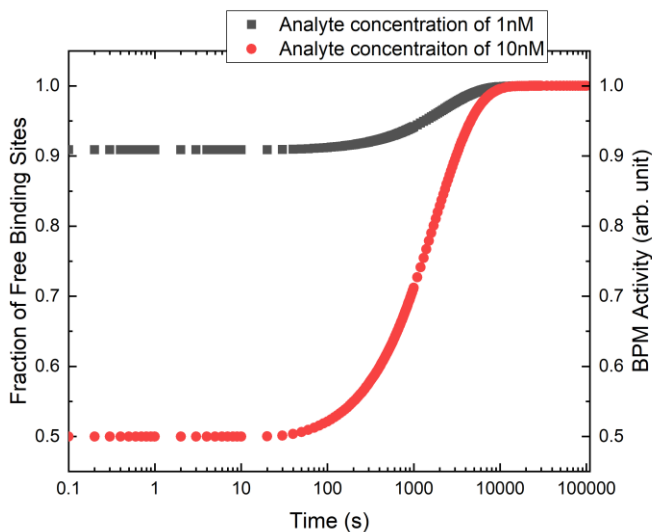
46

Figure 5.23: Development of the fraction of free binding sites and the relative BPM activity for reversing the BPM competition assay. In black the sensor is reversed from $1nM$ and in red from $10nM$ for the same reaction parameters: $K_d = 10^{-8}M$, $k_{off} = 10^{-3}s^{-1}$ and $k_{on}10^5M^{-1}s^{-1}$,

5.5 BPM SANDWICH ASSAY

In the previous section increases and decreases of the analyte concentration in BPM competition assays were discussed, as well as the influences of the reaction parameters k_{on}, k_{off} and K_d. In this section the responses of BPM sandwich assays will be discussed. As described in section 4.4 to the surface of the flow cell as well as to the surface of a particle binders are attached with which analyte can react. The relative activity will be determined for different sandwich assays for equal concentration in section 5.5.1. The time to reach equilibrium for different sandwich assays and different concentrations is discussed in section 5.5.2.

5.5.1 Simulated activity for different sandwich assays

For sandwich assays with K_d ranging from; 10^{-5}M$\leq K_{d,surface} \leq 10^{-9}$M and 10^{-8}M$\leq K_{d,particle} \leq 10^{-10}$M simulations are performed for an inflowing sample with an analyte concentration of $c_0 = 1$nM at $t = 0$. The initial concentration at $t = 0$ in the BPM flow cell is 0M.

The relative activities for 10^{-9}M$\leq K_{d,surface} \leq 10^{-5}$M and for 10^{-10}M$\leq K_{d,particle} \leq 10^{-8}$M are plotted in a bar diagram in figure 5.24. Region **V** from figure 2.3 is clearly visible for $K_d = c_0$ (the yellow bars). For $K_{d,surface} > c_0$ and increasing $K_{d,particle}$ the activity decreases, as illustrated as a transition form region **II** to region **I** in figure 2.3. The fraction of free binding sites on the particle increases for increasing K_d. The fraction of free binding sites is larger than $\frac{1}{2}$, thus the amount of combination of free and reacted binders decreases, hence the activity decreases.

For $K_{d,particle} < c_0$ and decreasing $K_{d,surface}$ the relative activity decreases as well. This corresponds to the transition from region **II** to region **III** in figure 2.3. The fraction of free binding sites decreases on the surface of the flow cell for decreasing $K_{d,surface}$. There are more reacted binders than free binders on the particle. Thus the amount of combination of free and reacted binders decreases, hence the activity decreases.

47

In contrast, for $K_{d,particle} > c_0$ and increasing $K_{d,surface}$ the relative activity increases. This corresponds to the transition from region **I** to region **IV** in figure 2.3. The fraction of free binding site decreases on the surface of the flow cell for decreasing $K_{d,surface}$. There are more free binders than reacted binders on the surface. Thus the amount of combinations of free and reacted binders increases, hence the activity increases.
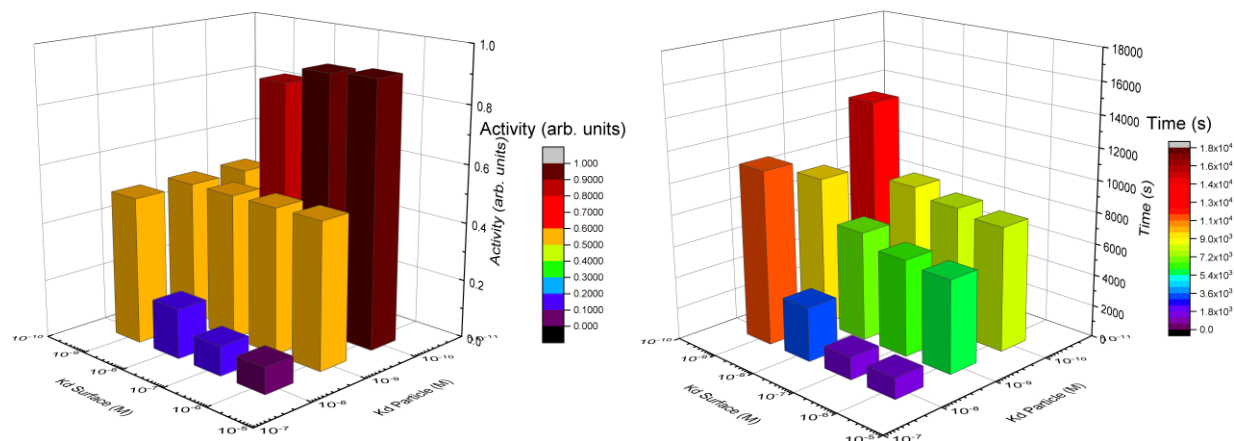

Figure 5.24: The relative activity of BPM sandwich assays, on the left, and the response times on the right, are plotted for an analyte concentration of 1nM, for $k_{on} = 10^6 M^{-1}s^{-1}$, $10^{-9}M \leq K_{d,surface} \leq 10^{-5}M$ and for $10^{-10}M \leq K_{d,particle} \leq 10^{-8}M$.

5.5.2   Time scale to reach equilibrium for sandwich assays

In this section the time scale on which different sandwich assays reach equilibrium will be discussed. Since in sandwich assays two different surfaces are reactive, that means that τ_r and Da from equation 30 are dependent on both. The timescales for different concentration but with equal activities will be analyzed. This is accomplished by scaling the K_d values with the analyte concentration, c_0. The concentration in the flow cell is 0M at $t = 0$. A sample with an analyte concentration flows into the geometry at $t = 0$. Simulations are performed for analyte concentrations of 10pM, 1nM and 100nM. For all simulation $k_{on} = 10^6 M^{-1}s^{-1}$ has been chosen for the reaction on the surface of the flow cell and the reaction on the surface of the particle. The k_{on} is kept equal, such that the Damköhler number for all simulation is equal. The Damköhler number has a value of 15, which implies that the simulated BPM sensor is in the transport limited regime and the timescale on which the system reaches equilibrium on one surface is $\tau_{CRD} = \tau_r Da$.

The relative activity for different values of $K_{d,surface}$ and $K_{d,particle}$ and the corresponding times on which 90% of the activity is reached for the simulations with an analyte concentration of 1nM, 100nM and 10pM are given in figures 5.24-5.26 respectively. The values for $K_{d,surface}$ and $K_{d,particle}$ are scaled for the analyte concentration of the sample. As discussed in section 5.5.1 the time to reach equilibrium decreases for decreasing K_d values.

As illustrated by figures 5.24-5.26, it takes longer to reach the same activity in equilibrium for lower concentrations. The same activity means that an equal amount of binders on the surface and the particle are reacted with analyte molecules in equilibrium. When the analyte concentration of the sample is low, it takes more time to reach equilibrium compared to samples with a high analyte concentration. Comparing the timescales of figures 5.24-5.26 it can be seen that the timescale to reach

48

equilibrium scales with $\sim 1/c_0$ between different concentration for similar equilibrium activities. The time constant on which equilibrium will be reached, τ_{CRD}, is proportional to the reaction time multiplied with the Damköhler number, $\tau_r Da$. The reaction time is proportional to $\frac{1}{k_{off}+k_{on}c_0}$ and the Damköhler number is proportional to k_{on}. The time constant, τ_{CRD}, should then be proportional to $\frac{1}{K_d+c_0}$.

The time after which an equilibrium activity of 0.1-0.2 is reached for an analyte concentration of 100 nM is relatively longer than for 1 nM and 10 pM. This implies that the shortest timescale on which the BPM sensor reaches equilibrium activity is the timescale to transport the sample from the patient to the surface and the particles. The timescale in the 100 nM regime is minutes. Visser et al. (2016) have performed measurements for 100 nM from which they have concluded that the timescale on which the BPM competition assay reaches equilibrium was in the order of 5 min. [21]

Simulation show that a time on the order of days is required to reach relative activities of 0.8-0.9 for an analyte concentration of 10 pM. However, the simulated timescales for activities of approximately 0.1 are on the order of hours. Visser et al. (2018) have performed BPM sandwich assay measurements in pM regime. The analyte concentration was increased in a stepwise fashion from 10 pM to 1000 pM. The activity was measured as function of the concentration. Unfortunately they concluded that their measurements were performed in a kinetic regime and not in thermal equilibrium. This implies that the timescale on which equilibrium would have been reached is longer than the times taken between the increases of the analyte concentration, which was 15 min. However, from their results it can be concluded that the timescale on which equilibrium is reached for 1000 pM, or 1 nM, is in the order of hours. It can be determined that for 1 nM a relative activity in the order of 0.9-1 was reached. From figure 5.24 it can be seen that the simulated timescale is the order of hours as well.

Figure 5.25: The relative activity of BPM sandwich assays, on the left, and the response times on the right, are plotted for an analyte concentration of $100nM$, for $k_{on} = 10^6 M^{-1}s^{-1}$, $10^{-7}M \leq K_{d,surface} \leq 10^{-3}M$ and for $10^{-8}M \leq K_{d,particle} \leq 10^{-6}M$.
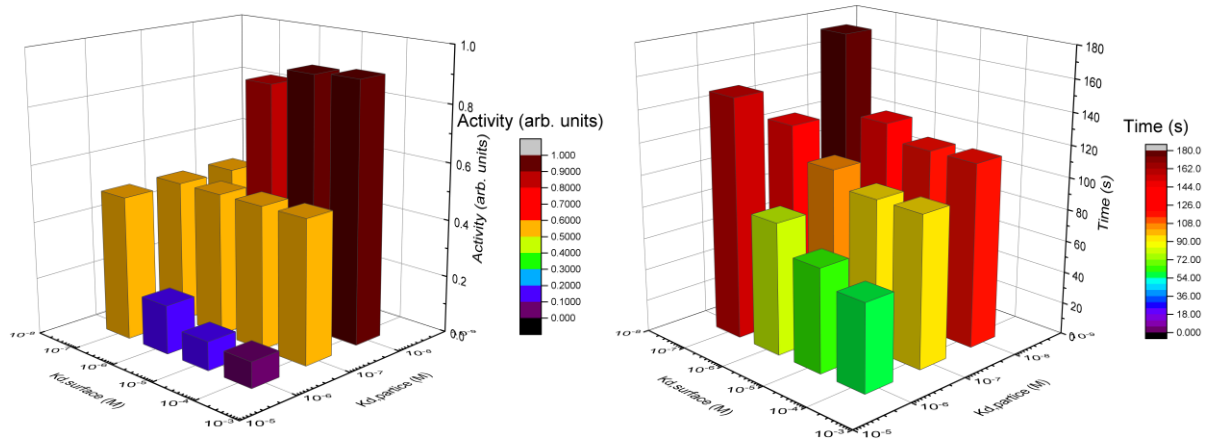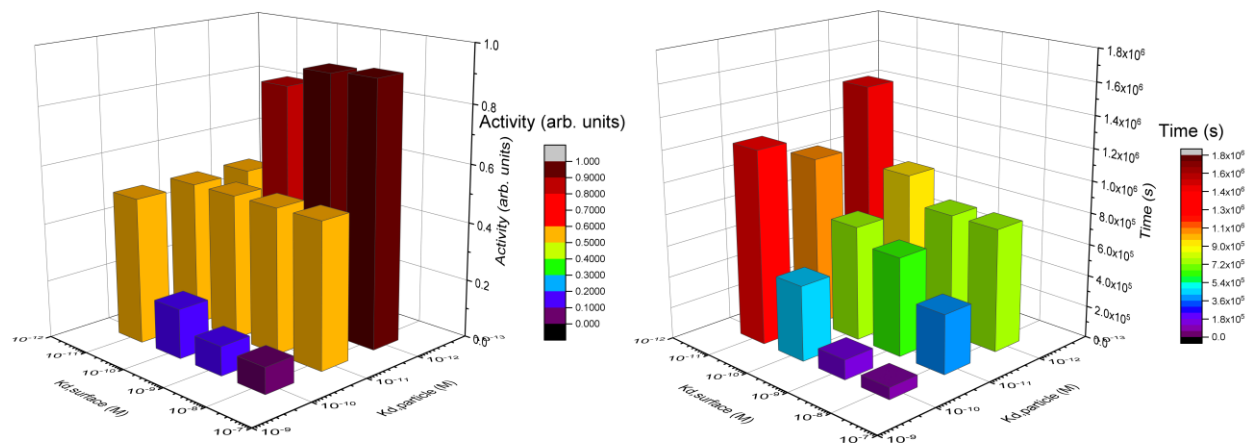
Figure 5.26: The relative activity of BPM sandwich assays, on the left, and the response times on the right, are plotted for an analyte concentration of $10pM$, for $k_{on} = 10^6 M^{-1} s^{-1}$, $10^{-11}M \leq K_{d,surface} \leq 10^{-7}M$ and for $10^{-12}M \leq K_{d,particle} \leq 10^{-10}M$.

6 CONCLUSION

Simulation were carried out to investigate the influence of advection, diffusion and reaction on the time dependent analyte concentration and the activity of the BPM sensor. By use of COMSOL Multiphysics a model was developed of the BPM sensor. The geometry was based on the recent BPM flow cell designs.

The time dependent analyte concentration between a particle and the surface has been studied by carrying out simulation with advection and diffusion. By studying the stream lines it was concluded that a fluid flow was present around a particle and underneath the particle. This implies that analyte would be transported by advection between the particle and the surface. Even though the particle has an influence on the fluid flow, it was simulated that a particle does not influence the timescale on which the analyte concentration increases between the particle and the surface. By comparing the time dependent analyte concentration simulated with and without diffusion, and by plotting the Péclet number near the particle, it was concluded that diffusion is dominant in the distribution of analyte molecules between the particle and the surface. Diffusion has a crucial role in the transport of analyte from the patient to the surface. The diffusion of analyte decreases the timescale on which the analyte concentration develops between the particle and the surface.

In early flow cell designs tube were connected to flow cell such that a distance between the backside of the flow cell and the tube was created. It was found that low flow speeds are present between the backside of the flow cell and tube compared to the flow speeds between the tube and the main flow chamber. It was concluded that the placement of the tube does not have an influence on the decrease of the analyte concentration. This implies that the measured experimental timescales are not caused by the placement of the tube relative to the backside of the flow cell.

The simplification was made to reduce the length of the tube, which connects the patient with the flow cell, from 20-50 cm to 0.1mm. To investigate the effect of a long tube, the influence of a tube length of 150mm was investigated. A longer tube causes the analyte concentration between a particle and the surface of the flow cell to increase later. For a longer tube more dispersion (stretching of the concentration profile) occurs, which will increase the time on which the analyte concentration develops. From the simulation with a tube length of 150 mm it was concluded that the simulated time required to transport the sample over the tube was correct. By simulating the tube with more and less mesh elements it was concluded that the simulated effect was not caused by the mesh.

A block pulse, with a width of 1 s, of analyte concentration was simulated in the BPM flow cell. The maximum of the time dependent analyte concentration near the surface was only 15% of the initial concentration of the pulse. Due to dispersion the pulse will be stretched in the direction of the flow. Since the amount of analyte should be conserved in the pulse the maximum analyte concentration of the pulse is decreased. It was found that the timescale on which the analyte concentration increased was short compared to the timescale on which the analyte concentration decreased. Due to the difference in flow speed between the side walls (width) of the flow cell and the center a concentration gradient is formed from the walls to the center. This slows down the decrease of the analyte concentration.

The influence of the reaction parameters k_{on}, k_{off} and K_d on the time dependent analyte concentration and the fraction of free binding sites for BPM competition assay was investigated. It was found that the analyte concentration increase in two phases. The timescale of the first phase is

transport dominated and the timescale of the second phase is reaction dominated. It was concluded that the fraction of free binding sites is only dependent on K_d. A lower K_d value will cause a lower fraction of free binding sites and also a lower activity. The timescale to reach an equilibrium fraction of free binding sites is dependent on the K_d value. Shorter timescales were calculated for higher K_d values. For similar K_d values but different k_{on} and k_{off} values it was calculated that there was a difference in the time required to reach the same equilibrium activity. For a flowrate of 30 µL/min and a binding site areal density of 10^{16} sites/m², it was concluded that for $k_{on} = 10^6$ M⁻¹s⁻¹ the timescale on which equilibrium was reached was twice as short as for $k_{on} = 10^5$ M⁻¹s⁻¹. However for $k_{on} > 10^6$ M⁻¹s⁻¹ the timescale to reach equilibrium should be independent on the k_{on} value. It was found as well that the depletion zone is unique for the k_{on} parameter. The depletion zone is maximum for $k_{on} > 10^6$ M⁻¹s⁻¹.

It was found that the decrease of analyte concentration also happens in two phases. The time of the first phase is dominated by transport of analyte and the time of the second phase is dominated by the reaction between analyte and binders. It was found that the time required to decrease to a analyte concentration of zeros is shorter for higher k_{off}, and for higher K_d values. It was concluded that the time required to decrease is longer than $1/k_{off}$, this is most likely caused by the rebinding of analyte molecules. The time required to decrease to a concentration of zero is unaffected by the initial analyte concentration of the system.

For different K_d values for the anayte binder reaction at the surface of the flow cell and the particle, the activity in equilibrium and the time to reach equilibrium were simulated. The activity is equal to 50% of the maximum value for surface $K_d = c_0$. Time to reach equilibrium increases for decreasing K_d values as seen for the competition assays. The time to reach equilibrium increases for decreasing concentration. The response time of the BPM sandwich assay scales with $1/c_0$. However for relative high concentration the response time of the BPM sandwich assay is equal to the time for the sample to be transported from the patient to the flow cell and to be distributed over the flow cell. The simulated timescale on which equilibrium is reached for 100 nM and 1 nM were of the same order as measured experimental timescales.

7 BIBLIOGRAPHY

[1]   Thévenot, D. R., Toth, K., Durst, R. A., & Wilson, G. S. (2001). Electrochemical biosensors: recommended definitions and classification. *Biosensors and bioelectronics*, *16*(1-2), 121-131.

[2]   Malhotra, B. D. (2017). *Biosensors: fundamentals and applications*. Smithers rapra.

[3]   Banica, F. G. (2012). *Chemical sensors and biosensors: fundamentals and applications*. John Wiley & Sons.

[4]   Mehrotra, P. (2016). Biosensors and their applications–A review. *Journal of oral biology and craniofacial research*, *6*(2), 153-159.

[5]   Martinkova, P., & Pohanka, M. (2015). Biosensors for blood glucose and diabetes diagnosis: evolution, construction, and current status. *Analytical Letters*, *48*(16), 2509-2532.

[6]   Mostafalou, S., & Abdollahi, M. (2017). Pesticides: an update of human exposure and toxicity. *Archives of toxicology*, *91*(2), 549-599.

[7]   Regulation on maximum residue levels of pesticides in or on food and feed of plant and animal origin and amending Council Directive 91/414/EEC, 396/2005 E.U. (2005)

[8]   Scognamiglio, V., Arduini, F., Palleschi, G., & Rea, G. (2014). Biosensing technology for sustainable food safety. *TrAC Trends in Analytical Chemistry*, *62*, 1-10.

[9]   Mastrototaro, J. J. (2000). The MiniMed continuous glucose monitoring system. *Diabetes technology & therapeutics*, *2*(1, Supplement 1), 13-18.

[10]   Visser, E. W., Yan, J., van IJzendoorn, L. J., & Prins, M. W. (2018). Continuous biomarker monitoring by particle mobility sensing with single molecule resolution. *Nature communications*, *9*(1), 1-10.

[11]   Bruus, H. (2008). *Theoretical microfluidics* (Vol. 18, pp. 346-346). Oxford: Oxford university press.

[12]   Squires, T. M., Messinger, R. J., & Manalis, S. R. (2008). Making it stick: convection, reaction and diffusion in surface-based biosensors. *Nature biotechnology*, *26*(4), 417-426.

[13]   Newman, J. (1973). The fundamental principles of current distribution and mass transport in electrochemical cells.

[14]   Ackerberg, R. C., Patel, R. D., & Gupta, S. K. (1978). The heat/mass transfer to a finite strip at small Péclet numbers. *Journal of Fluid Mechanics*, *86*(1), 49-65.

[15]   Griesmer, A. (2013, March 6). *What is COMSOL Multiphysics*. COMSOL. https://www.comsol.com/blogs/what-is-comsol-multiphysics/

[16]   Franchini, M., & Mannucci, P. M. (2012, February). Thrombin and cancer: from molecular basis to therapeutic implications. In *Seminars in thrombosis and hemostasis* (Vol. 38, No. 01, pp. 95-101). Thieme Medical Publishers.

[17]   Harmison, C. R., Landaburu, R. H., & Seegers, W. H. (1961). Some physicochemical properties of bovine thrombin. *Journal of Biological Chemistry*, *236*(6), 1693-1696.

[18]   Yan, J., van Smeden, L., Merkx, M., Zijlstra, P., & Prins, M. W. (2020). Continuous Small-Molecule Monitoring with a Digital Single-Particle Switch. *ACS sensors*, *5*(4), 1168-1176.

[19]   Yang, K., Li, M., Ling, N. N., May, E. F., Connolly, P. R., Esteban, L., ... & Johns, M. L. (2019). Quantitative tortuosity measurements of carbonate rocks using pulsed field gradient nmr. *Transport in Porous Media*, *130*(3), 847-865.

[20]   Perkins, T. K., & Johnston, O. C. (1963). A review of diffusion and dispersion in porous media. *Society of Petroleum Engineers Journal*, *3*(01), 70-84.

[21]   Visser, E. W. Biosensing Based on Tethered Particle Motion. PhD thesis. Technical University Eindhoven, 2016. 6, 19

[22]   Di Cera, E. (2008). Thrombin. *Molecular aspects of medicine*, *29*(4), 203-254.

[23]   Visser, E. W., van IJzendoorn, L. J., & Prins, M. W. (2016). Particle motion analysis reveals nanoscale bond characteristics and enhances dynamic range for biosensing. *ACS nano*, *10*(3), 3093-3101.

APPENDICES

A: TIME REQUIRED TO INCREASE FROM ZERO TO DIFFERENT ANALYTE CONCENTRATION

Simulations were carried out to show that the time required to increase scale with the concentration gradient. The initial analyte concentration is zero and at $t = 0$ a sample flows into the flow cell. The time dependent analyte concentration is measured between a particle and the surface of the flow cell. In figure A.1 the development of the time dependent normalized analyte concentration is plotted over the time for samples with analyte concentrations of 1 nM, 1 µM and 1 mM. The local analyte concentration starts at the initial concentration of 0M before developing at $t = 11$ s. For all three simulation after $t = 22$ s the local analyte concentration reaches the analyte concentration of the sample and the sample has been locally distributed around the particle. It can be seen that independent of the sample's analyte concentration the time required to increase is scaled for the concentration gradient.
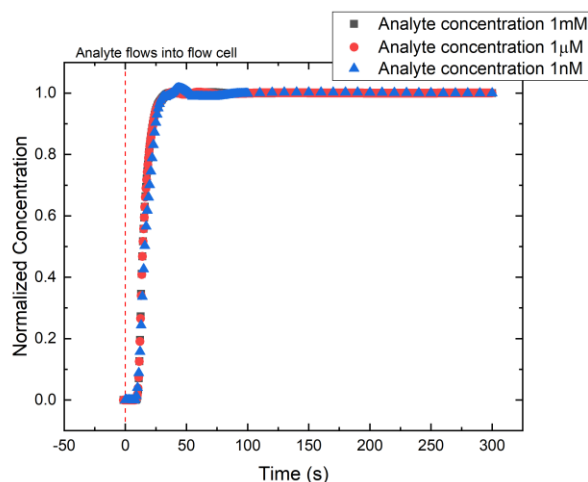

Figure A.1: Time development of increasing analyte concentration close above the surface, plotted for normalized concentration. The curves come together on one curve, meaning that the distribution of the sample scales with the analyte concentration. In black the analyte concentration of the sample was 1mM, in red 1µM and in blue 1nM.